Minerals **2012**, *1*, 169-207; doi:10.3390/min2030169

OPEN ACCESS

minerals

ISSN 2075-163X

www.mdpi.com/journal/minerals/

Article

Zn-Pb Ores of Mississippi Valley Type in the Lycksele-Storuman District, Northern Sweden: A Possible Rift-Related Cambrian Mineralisation Event

Kjell Billström [1,*], Curt Broman [2], Jens Schneider [3], Warren Pratt [4] and Göran Skogsmo [5]

[1] Laboratory for Isotope Geology, Swedish Museum of Natural History, Stockholm SE-10405, Sweden

[2] Department of Geological Sciences, Stockholm University, Stockholm SE-10691, Sweden; E-Mail: Curt.Broman@geo.su.se

[3] Freiberg School of Mines, Freiberg 09596, Germany; E-Mail: J.Schneider@mineral.tu-freiberg.de

[4] Specialized Geological Mapping Ltd., Catlin Cottage, Station Rd, Urquhart Moray, Elgin IV30 8LQ, UK; E-Mail: pratt_warren@yahoo.co.uk

[5] Björka Mineral AB, Björkaverken, Glanshammar SE-705 97, Sweden; E-Mail: Goran.Skogsmo@omya.com

* Author to whom correspondence should be addressed; E-Mail: Kjell.Billstrom@nrm.se; Tel.: +46-8-519-551-28; Fax: +46-8-519-651-30.

Received: 30 March 2012; in revised form: 7 June 2012 / Accepted: 20 June 2012 / Published: 29 June 2012

Abstract: The epigenetic Zn-Pb deposits in the Lycksele-Storuman ore district, northern Sweden, are hosted by Paleoproterozoic basement near the margin of the Caledonian mountains. A paleogeographic reconstruction suggests that platform sediments, including Cambrian shales, overlaid the mineralised basement. The mineralisation type, containing sphalerite, galena, calcite and fluorite, is confined to veins and breccias and interpreted to be of Mississippi Valley Type (MVT) style. There is no appreciable wall rock alteration. Fluid inclusion work reveals coexisting aqueous and hydrocarbon fluids. Ore deposition is interpreted to have occurred during mixing of two fluids; a cool (<70 °C) brine with a salinity of 30 eq. mass% $CaCl_2$ and a hot (~200 °C) brine with about 18 eq. mass% $CaCl_2$. The mixing led to complex Sr isotope systematics in the analysed minerals. A tentative sphalerite Rb-Sr isochron age of a 534 ± 13 Ma probably dates mineralisation. The isotope systematics of Pb and Nd are less complex and both elements were essentially leached

from basement rocks and transported by the hot fluid. Ore formation is considered to have taken place during rifting, related to the opening of the Iapetus Ocean.

Keywords: Zn-Pb mineralisation; cambrian; rifting; fluid inclusions; ages; isotopic tracers

1. Introduction

Recent prospecting discovered several epigenetic, fracture-controlled zinc- and lead-rich sulphide deposits along the Caledonian mountains in northern Sweden. The deposits are hosted by early Proterozoic basement and represent an ore type not described in detail before in northern Sweden. The studied deposits are located in the Lycksele-Storuman ore district, a NW-trending belt, approximately 40–50 km wide and more than 100 km long (Figure 1). Also known as the 'Gold Line', it occurs between the Caledonian (0.5–0.4 Ga) orogen in the west and the early Proterozoic (1.9 Ga) Skellefte VHMS district in the east. Relatively little is known about the detailed geological evolution in the Lycksele-Storuman ore district, except that it carries a range of ore types, including orogenic Au, VHMS, U, Sn-W, and Zn-Pb mineralisation. This paper focuses on fracture-controlled Zn-Pb deposits, characterised by open-space fillings of breccias and fractures mainly within >1.8 Ga metasedimentary rocks. In particular, the study is concentrated on the geology of the Ersmarksberget and Svärtträsk deposits, operated by Scan Mining between 2006 and 2007, and with estimated overall ore reserves amounting to approximately 10 Mton [1].

The origin of these Zn-Pb ores is enigmatic and there was no attempt to categorise Ersmarksberget and Svärtträsk in the recent Skellefte District memoir [2]. Given its economic potential and the poor understanding of the geological context, this article aims to elucidate the genesis of this type of Zn-Pb mineralisation. The epigenetic ore is clearly younger than *ca.* 1.8 Ga, since it is hosted by rocks of that age. The proximity of the deposits to the Caledonian mountain range (Figure 1), which includes autochthonous Lower Cambrian sedimentary rocks unconformably overlying Proterozoic basement, suggests a possible link to the Caledonian orogeny or an earlier event. The Lower Cambrian rocks host important sandstone-hosted Zn-Pb ores (e.g., Laisvall [3]), which share several features with the Zn-Pb ores of the Lycksele-Storuman district. There are also other examples of Caledonian vein mineralisation, which need to be considered in a genetic framework.

Ore mineralogy and analytical results of the studied Zn-Pb ores are comparable with Mississippi Valley Type (MVT) mineralisation and, although the host rocks are not the classic carbonates that host most MVT deposits, we interpret the Zn-Pb deposits in the Lycksele-Storuman district as an unusual, fracture-controlled MVT deposit. This deposit type is known to be notoriously difficult to date and both palaeomagnetic and isotopic methods have been applied. In the present study, Rb-Sr isotope dating was applied to sphalerite in order to constrain the age of ore formation. Furthermore, samples were collected for fluid inclusion and isotopic (Pb, Sr and Nd) analysis of the ore-bearing assemblages to characterise the mineralising fluids and investigate the source of metals.

Figure 1. Simplified geological map of the Lycksele-Storuman Ore District (LSOD). The LSOD is approximately confined to the area between the dashed lines. The study areas are indicated by small boxes (Figures 2–4). This figure and Figures 2a, 3 and 4 are modified after the digital map databases of the Geological Survey of Sweden (SGU). Coordinates refer to the Swedish National Grid, RT 90. Inset map: Location of LSOD in northern Sweden. SOD = Skellefte Ore District. NOD = Norrbotten Ore District.

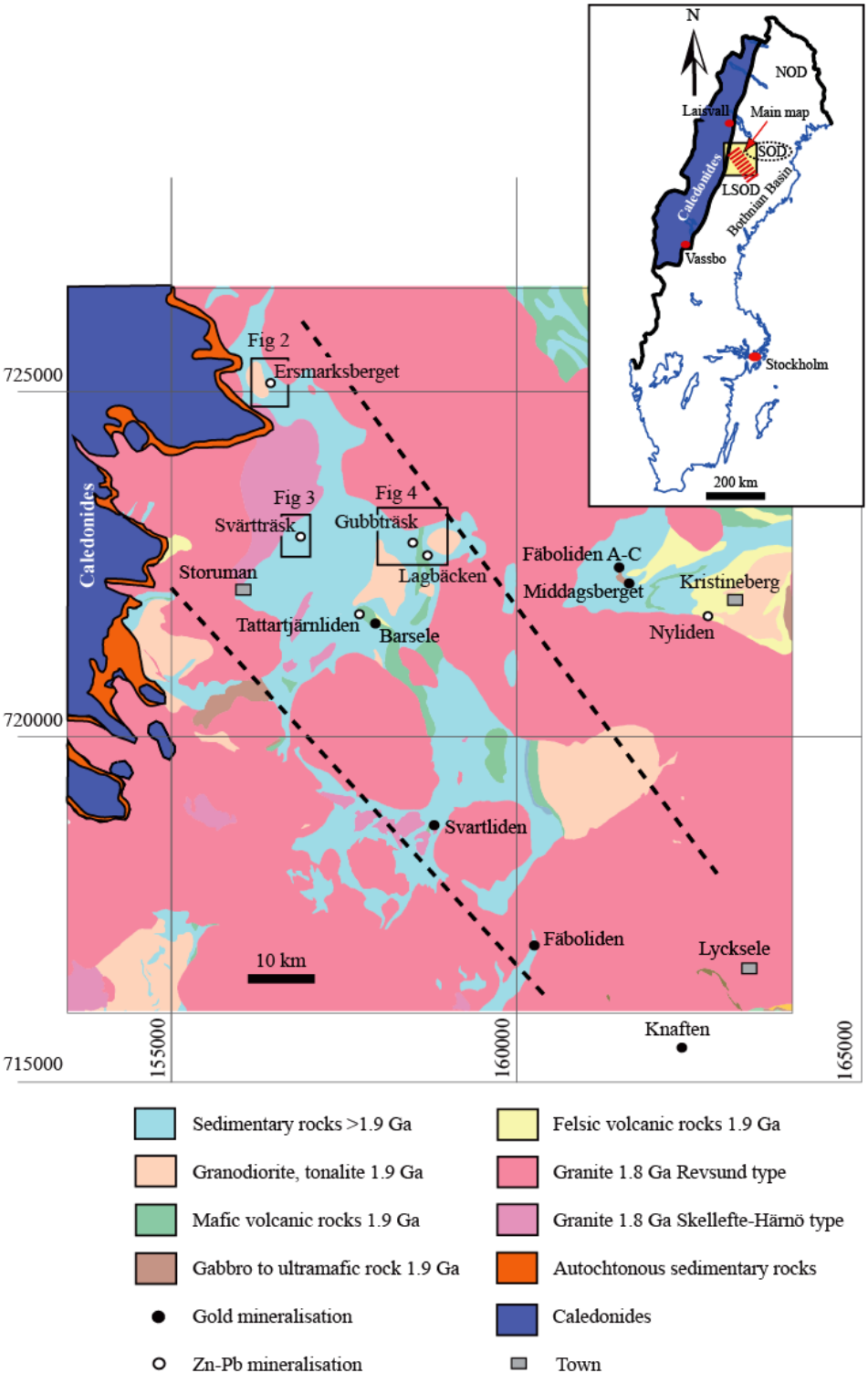

2. Geology

2.1. Regional Geology

The study area is located in northern Sweden (Figure 1), within the Fennoscandian Shield. In palaeogeographic reconstructions this is sometimes referred to as Baltica; it forms the north-western part of the East European craton and constitutes large parts of Finland, north-west Russia, Norway, and Sweden. The bedrock in the shield shows north-east to south-west crustal growth, reflected by Archean rocks in the north-east and successively younger rocks towards the south-west [4]. Large parts of northern Sweden comprise so-called 'Svecofennian' rocks, formed during the Svecokarelian orogeny at 1.96–1.8 Ga [5]. This orogeny produced ≥1.9 Ga island arc terranes that were intruded by different generations of granitoids.

The Skellefte district comprises VHMS ores located within a 120 × 30 km belt of 1.89 to 1.88 Ga early Proterozoic rocks. The massive sulphide ores are hosted by marine volcanic rocks of the Skellefte Group, interpreted as a volcanic arc that underwent subsequent extension [6,7]. The mineralised belt is bordered by a large marine basin in the south which is dominated by metasedimentary rocks (Bothnian Group) and abundant granitoids.

Bark and Weihed [8] used the name 'Lycksele-Storuman ore district' for the area west of the better-known 1.9 Ga Skellefte massive sulphide ore district (SOD in Figure 1). Both districts have similar rock types, but there are important distinctions; the Lycksele-Storuman district is not simply a westerly extension of the Skellefte district. The Lycksele-Storuman ore district (LSOD) comprises mainly Bothnian metasedimentary rocks (*ca.* 1.96–1.86 Ga), with minor volcanic rocks (Figure 1). These are surrounded by large batholiths of late- to post-orogenic, 1.8 Ga granite (Revsund granite), and similarly aged granitoids of the Sorsele and Skellefte-Härnö suites. The metallogeny of the LSOD is diversified [2]; it includes orogenic Au deposits, e.g., Fäboliden [8], Zn-Pb ores (Ersmarksberget), minor massive sulphide (Barsele), U (Duobblon), and Sn-W mineralisation (Tvåtjärnmyran).

Apart from regional bedrock mapping by the Geological Survey of Sweden and limited prospecting work by mining companies, no systematic field work has been carried out in the LSOD. Little is known about the rock stratigraphy because the large Revsund granite massifs obscure field relationships. Major regional deformation and metamorphic events, as well as the emplacement of the Skellefte-Härnö and the Revsund granitoids, took place at about 1.85–1.80 Ga [2,9]. After peak metamorphism, shear zones oriented along a roughly N-S direction were developed in the area [9].

A thin Late Precambrian to Lower Cambrian sequence was deposited on the Proterozoic basement rocks. These rocks are largely eroded now and preserved only as a narrow rim along the Caledonian margin (Figure 1). This sequence comprises sandstones and shales [10,11], deposited in response to opening of the Iapetus Ocean. These units are overlain by the Alum Shale Formation, which comprises organic-rich (10%–20% by weight) and pyrite-bearing carbonaceous shale [12]. This shale represents strongly anoxic conditions, dominated by clay deposition and accumulation of limestones [11,12].

At approximately 0.5 to 0.4 Ga, the closure of the Iapetus Ocean triggered the Caledonian orogeny. During this orogeny, several allochthonous nappes thrust over the autochthonous Cambrian sedimentary rocks. The Alum Shale, may have acted as a tectonic detachment zone for the thrusting [13], and was strongly sheared [10].

2.2. Mineralization in the Lycksele-Storuman District

Zinc-lead mineralisation was studied at the Ersmarksberget, Svärtträsk, Gubbträsk and Lagbäcken occurrences along a narrow NW-SE zone in the LSOD (Figure 1). Lack of exposure limits detailed geological mapping, but the open pit at Ersmarksberget allowed detailed mapping and a clear picture of structural controls on ore. Apart from the Revsund, Sorsele- and Skellefte-Härnö granitoids, which suffered only weak metamorphism, all rocks have been subjected to greenschist-amphibolite metamorphism. However, for simplicity, the prefix meta- is omitted below.

2.2.1. Ersmarksberget

This Zn-Pb-Au deposit (also referred to as Blaiken), located 30 km N of Storuman (Figure 1), is mined as a series of narrow pits along the contact between a large mass of igneous rock (Juktan Dome) and metamorphosed Bothnian sedimentary rocks (Figure 2a). Most rocks are structureless siltstones, graphitic silty mudstones, and massive sandstones and greywackes. Rare augen of marble, up to 0.5 m wide, also occur. There are also common slumped silty mudstones with contorted siltstone and sandstone clots. All the Bothnian rocks, particularly the graphitic mudstones, are rich in pyrrhotite and pyrite. The younging direction is uncertain, but rare cleavage/bedding relationships suggest it is northwards and that the strata are the right way up.

There is a great variety of igneous rocks at Ersmarksberget, mostly as narrow sheared augen (Figure 2b). Igneous textures are preserved away from high strain zones and in the core of larger augen. They may have been dykes or sills, or portions of large plutons incorporated into shear zones. Whatever their original geometry, the range and variety is remarkable and includes: equigranular and medium-grained diorites and quartz diorites; coarsely porphyritic gabbro and diabase; coarse-grained amphibolites with actinolite-tremolite and albite. At their contacts, the amphibolites become more strongly foliated and biotite-rich, reflecting increased contact strain. Rare augen of tremolite and sulphide-rich rocks, mostly <0.5 m wide, are probably original ultrabasic intrusions. The Juktan Dome, immediately W of the pits (Figure 2a,b), has a dacitic-tonalitic composition. It has dimensions of about 4 × 2 km, elongated approximately north-south. The border of the Juktan Dome comprises dacite with abundant plagioclase and hornblende, and scattered blue quartz phenocrysts. Another large dacite outcrop is located northwest of the Dome; since none of these rocks resemble typical plutonic rocks, they are best interpreted as sub-volcanic intrusions.

Structural work at Ersmarksberget indicates two main deformation events; however, as there is no structural framework for the region, it is unclear how these events relate to regional structures. The entire sequence suffered strong ductile deformation (D_1), under greenschist conditions. Compression was broadly E–W. The mudrocks developed a strong stretching lineation, plunging moderately N, and subvertical slaty cleavage. Metamorphic minerals include biotite in basic rocks and rare andalusite (chiastolite) in the mudrocks. Clots of pyrrhotite, pyrite and arsenopyrite are boudinaged and display necks of coarse biotite in places. The deformation was strongly partitioned; the larger acid intrusions, in particular the Juktan Dome, acted as rigid bodies and the regional foliation intensifies toward them, and wraps around the bodies. The contact of the Juktan Dome is also folded; these folds have axial planar S_1 foliation in the mudrocks.

Figure 2. (**a**) Geological map of the Ersmarksberget Zn-Pb deposit and its surroundings; (**b**) Detailed geological map of part of the Ersmarksberget open pit showing the distribution of visible Zn/Pb mineralisation usually hosted by minor faults (certain zones with manifested abundance of one or several of the following phases; sphalerite, galena and fluorite are outlined). Sampling was carried out at similar sites in the mudstone along the eastern Juktan Dome contact. Coordinates in Figures 2–4 refer to the Swedish National Grid, RT 90.

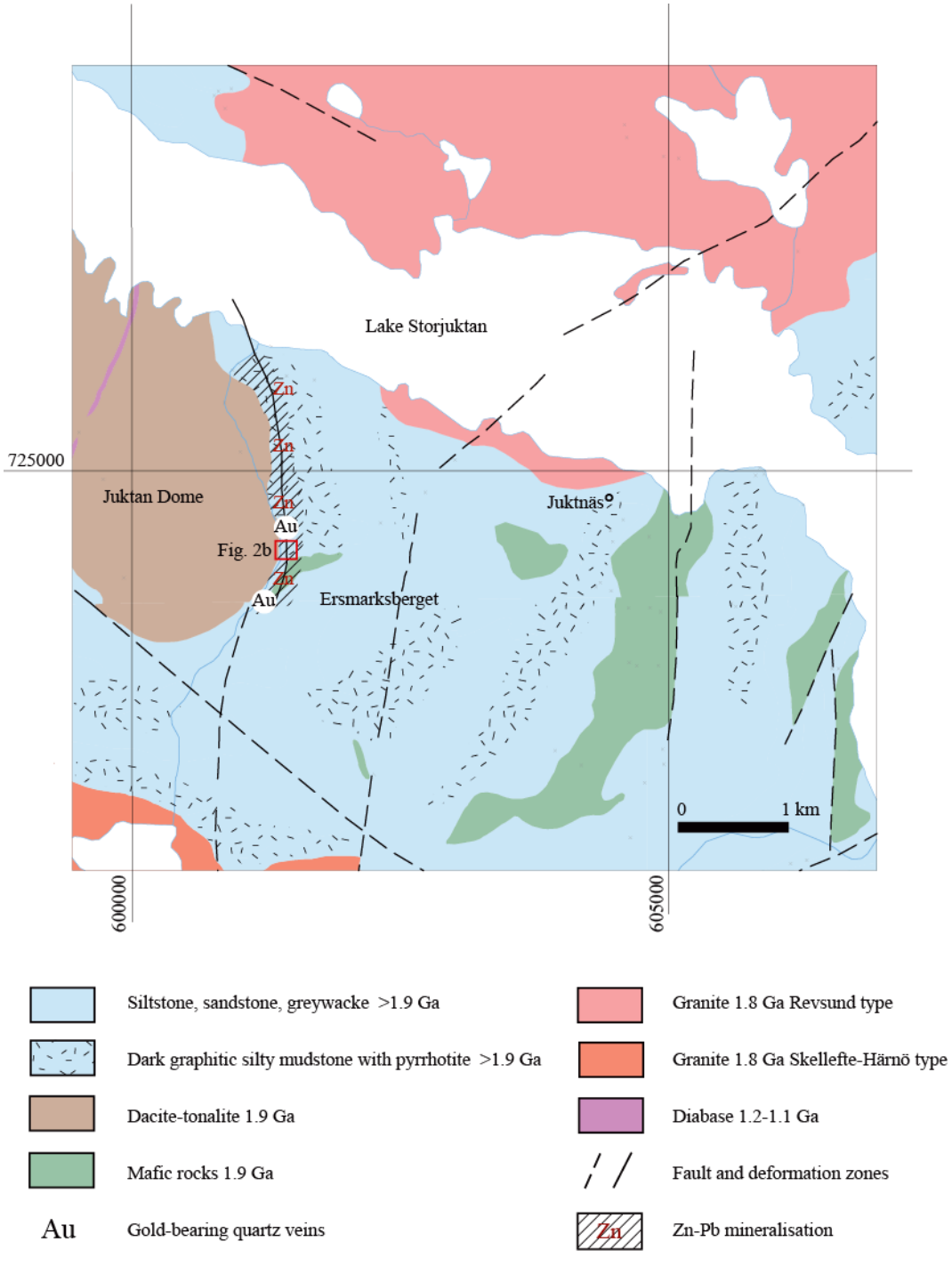

(a)

Figure 2. *Cont.*

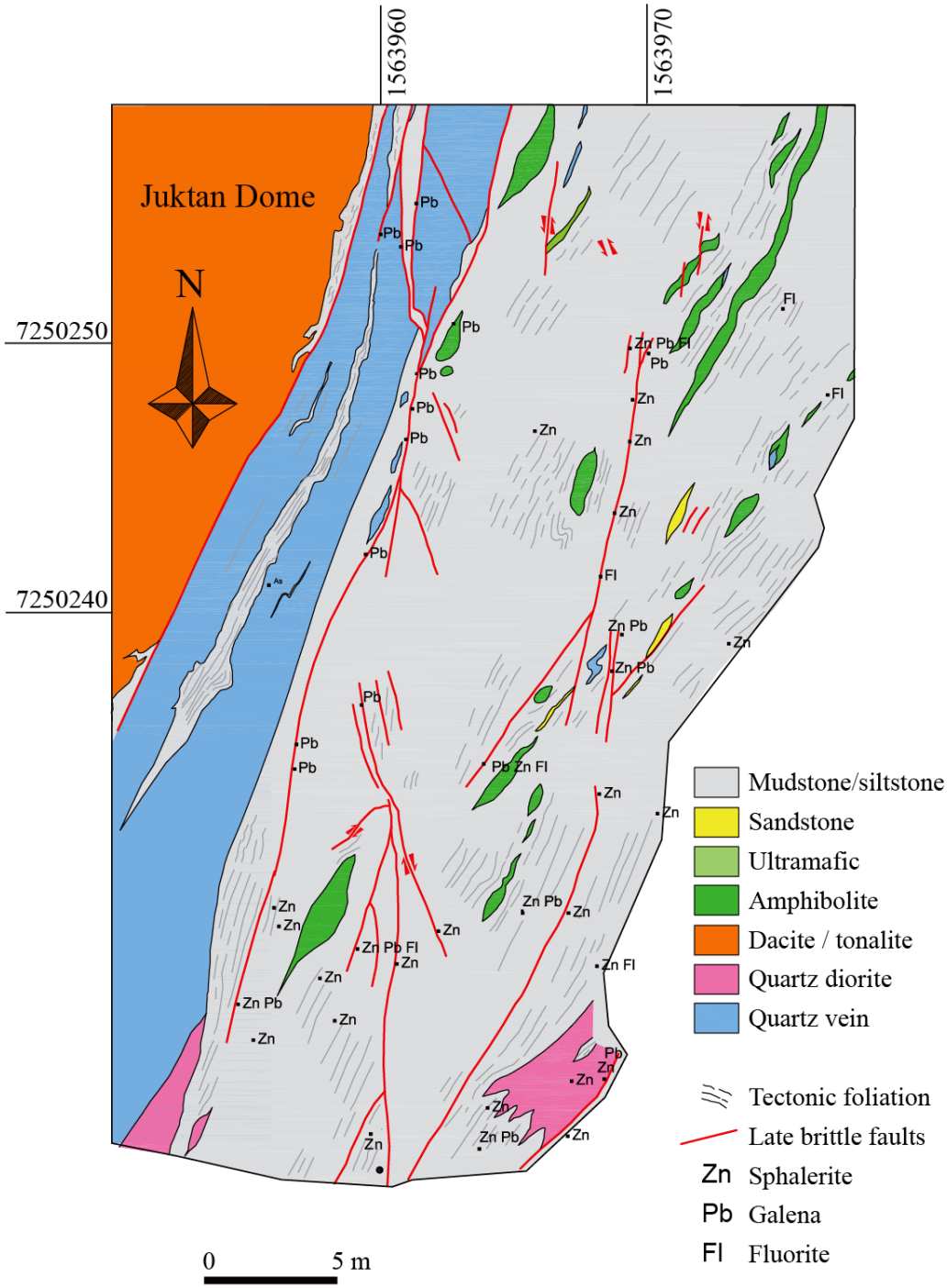

(b)

Intrusive rocks in the mudrocks were strongly boudinaged; quartz vein necks occur in the more competent acid intrusions, whereas basic intrusions form elongate augen without necks (Figure 2b). Away from the contact of the Juktan Dome, blobs of sandstone within the slumped mudrocks are progressively less stretched and igneous intrusions less boudinaged. A major milky quartz vein with arsenopyrite occurs at the Juktan Dome contact for a strike-length of at least 300 m. Up to 10 m thick, it contains anastomosing ribbons of, and interfingers with, graphitic mudstones. This major quartz vein

hosts Au and is interpreted as a local D_1 detachment between the Juktan Dome and the ductile, graphitic Bothnian mudrocks.

Most Zn-Pb mineralisation at Ersmarksberget comprises mineralised late brittle (D_2) faults and swarms of sphalerite-galena veinlets. Economic ore bodies occur where veinlet frequency increases sufficiently. The veins cut across D_1 quartz and arsenopyrite veins and across F_1 folds. There is abundant evidence that Zn-Pb-Ag-Au were deposited in dilational sites and at the intersections of faults. The brittle faults have clear strike-slip offsets and dilations occur where they change direction, intersect, or cut a more competent rock. In the most brittle host rocks, such as the Au-bearing quartz vein, open spaces are part-filled by crustiform veins comprising zoned sphalerite, galena, fluorite, siderite and calcite. A final event comprises botroyoidal marcasite and fine pyrite, locally as 'stalactites' in open spaces. These stalactites pitch steeply north or are vertical, suggesting that the mineralised system has not been significantly tilted. Rare chalcedony occurs in some veinlets. There is very little wallrock alteration around the veins. Crenulations and F_2 drag folds caused by faulting are widespread. They display consistent asymmetry and have saddle reefs and axial planar veinlets of quartz, sphalerite, galena, siderite and fluorite, less commonly chalcopyrite. Some drag folds pass directly into mineralised faults. Overall, it is very clear that the crenulation cleavages are related to drag folding on faults and that they developed at the same time as mineralisation.

There are several mineralised fault directions, each showing different offsets. Close to the Juktan Dome, the major faults are mostly parallel to the contact. Over much of its length, this contact comprises a soft gouge, up to 0.5 m thick, rich in crushed quartz vein and graphitic mudstone fragments. Rare blocks of sheared galena occur in the gouge, indicating some post-mineral movements. Offsets are largely sinistral; some sinistral dilational jogs are filled by gouge. These major faults locally offset, or repeat, the major quartz-Au vein. The best accumulations of sphalerite and galena occur within dilations, for example, where faults bend or are offset. However, the faults close to a N-S orientation have been reactivated and the sulphides milled. A significant N-striking mineralised fault, referred to as the "Purple Fault" because of the quantity of purple fluorite, branches from the Juktan Dome contact. This sinuous fault shows common splays and jogs implying a component of sinistral strike-slip. The fault hosts Zn-Pb mineralisation, but unusually for Ersmarksberget, also gives Au values up to several grams/tonne (g/t). There are also subsidiary sphalerite-mineralised north-northwest-striking, subvertical faults. They have mainly sinistral offsets and are probably horsetail splays from the main north-striking sinistral set. An important NE-striking set of sphalerite-mineralised faults, with steep to moderate north dips, has mainly dextral offsets.

In summary, Pb-Zn mineralisation at Ersmarksberget is near-surface and associated with brittle faults and there is no indication of Zn-Pb mineralisation during D1. This faulting had a strong component of strike-slip, with sinistral offsets on the principal north-striking faults. Overall, the deformation appears be either sinistral strike-slip or transtensional (with sinistral and extensional components). Zn-Pb-mineralised brittle-ductile structures, which clearly post-date the 1.8 Ga Svecofennian schistosity, were focused close to the Juktan Dome contact. Dilational jogs formed important, vertically plunging oreshoots.

2.2.2. Svärtträsk

The Svärträsk deposit (also referred to as the Hemberget occurrence) occurs 9 km NE of Storuman and is similar to Ersmarksberget. It is hosted by graphite- and pyrrhotite-bearing mudrocks and greywackes (Figure 3). Due to deformation and poor exposure, it is not possible to correlate the lithostratigraphy between the two deposits. The ore occurs within lens-shaped bodies, with thicknesses between 5 m and 60 m, in a zone at least 900 m long [2]. This zone is a NE-NNE-striking quartz-breccia zone that dips steeply SE. Reddish sphalerite and minor galena occur in small irregular quartz-calcite veinlets. Less than 2 km away from the Zn-Pb zone, close to a Revsund-type granite, there is skarn-type scheelite mineralisation. This occurs in a steeply dipping, disc-shaped 5–12 m layer of hornblendite.

Figure 3. Geological map of the area around the Svärtträsk Zn-Pb deposit.

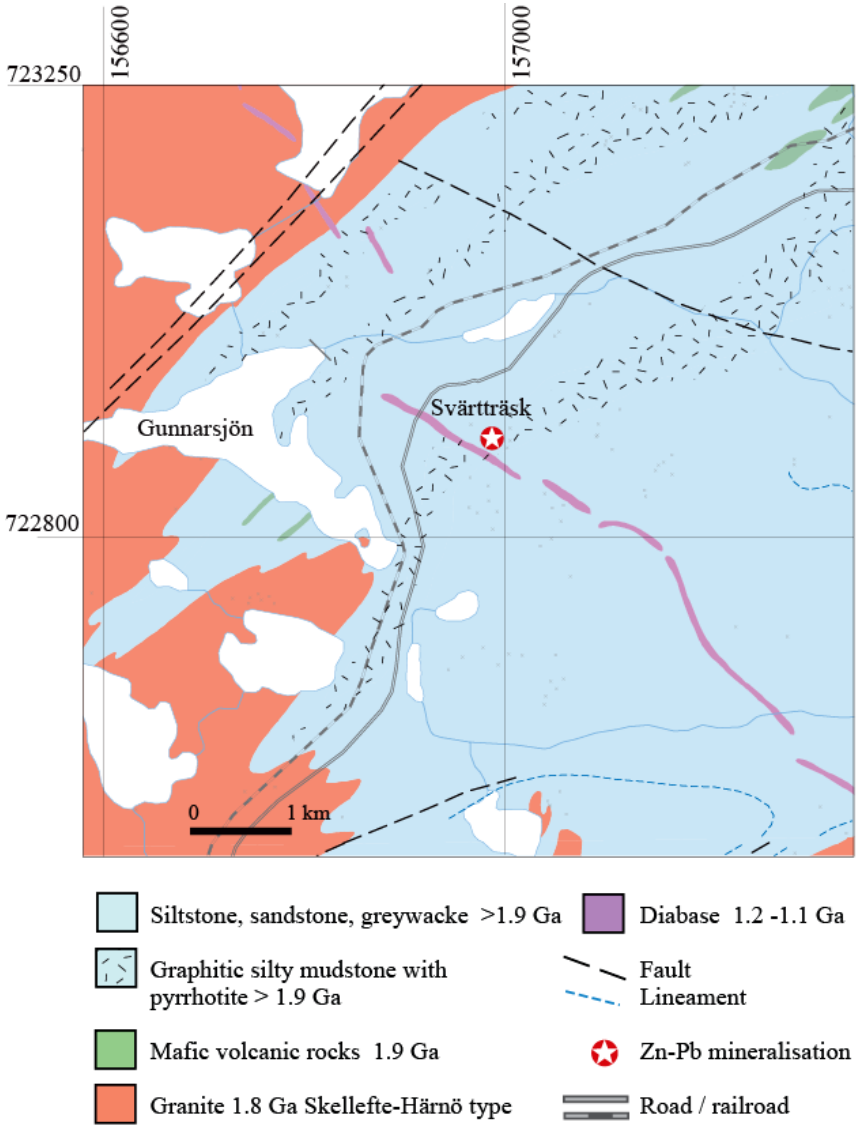

2.2.3. Gubbträsk

Geological information for the Gubbträsk mineralisation, about 30 km southeast of Storuman, is mostly based on drill core and data that is summarised in an unpublished report [14]. The bedrock comprises deformed turbiditic greywackes and mudstones, with units of basalt and andesite [15]. A 1.8 Ga Skellefte-Härnö granite occurs nearby; Revsund-type granitoids are widespread further north (Figure 4).

Two ore types were distinguished [14]; Au-bearing zones along ductile structures and breccia-style mineralisation carrying sphalerite and galena. The first is thought to be early Proterozoic and is similar to the Fäboliden gold mineralisation [8]. It includes arsenopyrite and pyrrhotite and occurs as quartz veins that are parallel to the regional foliation (NE-SW). The Zn-Pb sulphides occur along structures discordant to the regional foliation, which could correspond to a brittle, drag-fold type crenulation as observed at Ersmarksberget. Calcite and quartz occur as gangue minerals, and, although calcite is more abundant, the highest ore grades are found in quartz-rich veinlets. It is possible that quartz is a remnant from the older (Au) system whilst calcite was deposited together with sphalerite and galena. Thus, at sites where the Au-bearing system was overprinted by brittle deformation, Zn-Pb sulphides were deposited.

2.2.4. Lagbäcken

The geology of this area (Figure 4), situated a few km south of Gubbträsk, is based only on drill core. The host rocks comprise turbiditic greywackes, metamorphosed mafic volcanic rocks, and granodioritic-tonalitic intrusions. Unlike Gubbträsk, where Zn is the most important metal, Pb-Ag mineralisation (Ag-rich galena) occurs at Lagbäcken. The mineralisation is mainly hosted in fractures and breccias in the intrusive rocks. Fourteen diamond boreholes show economic mineralisation for a length of 150 m in a N-S direction, which is indicated to a depth of at least 100 m. The drillhole results include 6 m at 6.6% Pb and 59.7 g/t Ag. This is part of a 23 m intersection with 2.2% Pb and 19.9 g/t Ag. Although based on information from only one drillhole, two sets of steeply dipping calcite-dominated veins may be defined. One is N-S oriented; the other strikes NE-SW. There is also evidence of early arsenopyrite-tourmaline mineralisation.

2.2.5. Tattartjärnliden and Nyliden

A few additional samples were taken from the two similar occurrences at Tattartjärnliden and Nyliden (Figure 1). The Tattartjärnliden samples consist of sphalerite and calcite veins and breccias in a deformed greywacke; the Nyliden samples comprise thin sphalerite and calcite veins in a graphitic siltstone.

2.2.6. Summary of Features Characteristic of Mineralized Samples

All the Zn-Pb occurrences comprise simple mineral assemblages of sphalerite, galena, calcite and fluorite (Figure 5) and occur typically as veinlets, in breccia zones and along faults and can be described as fracture-controlled. In places, where strongly fractured, mineralisation forms the cement in stockworks and the breccia matrix. There is abundant evidence of growth within open spaces. The veins are generally thin (<10 mm), but open spaces at intersections of fractures are wider. Both

veinlets and breccia fragments have sharp margins and there is no appreciable alteration halo. There is no evidence of explosive hydrothermal activity, and ore deposition was remarkably passive. The sphalerite normally consists of coarse crystals, but spherulitic sphalerite is also present (Figure 6). Galena is commonly intergrown with sphalerite, but several tiny veinlets contain only sphalerite. In places, open vugs are partly filled by coarse sphalerite crystals. Sphalerite was clearly deposited early in the paragenesis. Coarse-grained white to grayish calcite is intergrown with sphalerite, but occurs mostly as overgrowths on sphalerite or as monomineralic cement in breccias and thin veinlets. Fluorite is late and fills the largest open spaces. Fluorite occurs as large crystals and can be colourless, violet and green. In some fluorite-rich veins, black hydrocarbons occur as crust or in vugs. In a few places corroded early quartz crystals are overgrown by sphalerite (Figure 7).

Figure 4. Geological map of the area enclosing the Zn-Pb occurrences at Gubbträsk and Lagbäcken.

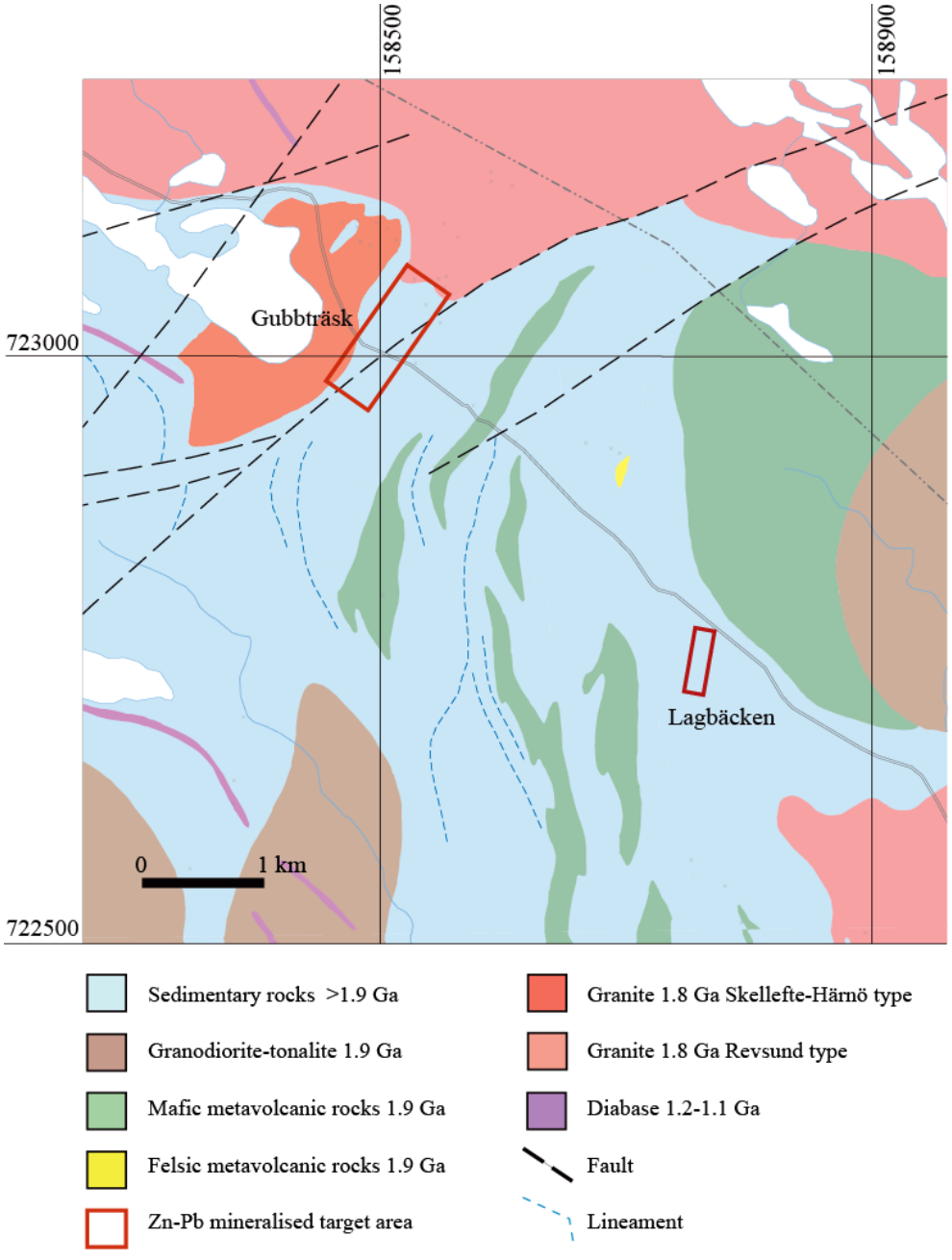

Figure 5. Typical samples of the studied fracture-controlled Zn-Pb mineralisation: (**a**) breccia-like fractures with sphalerite in a calcite cement (Lagbäcken); (**b**) sphalerite-filled open space with intergrown calcite followed by an overgrowth of coarse-grained calcite (Gubbträsk); (**c**) breccia with coarse-grained sphalerite cement (Ersmarksberget).

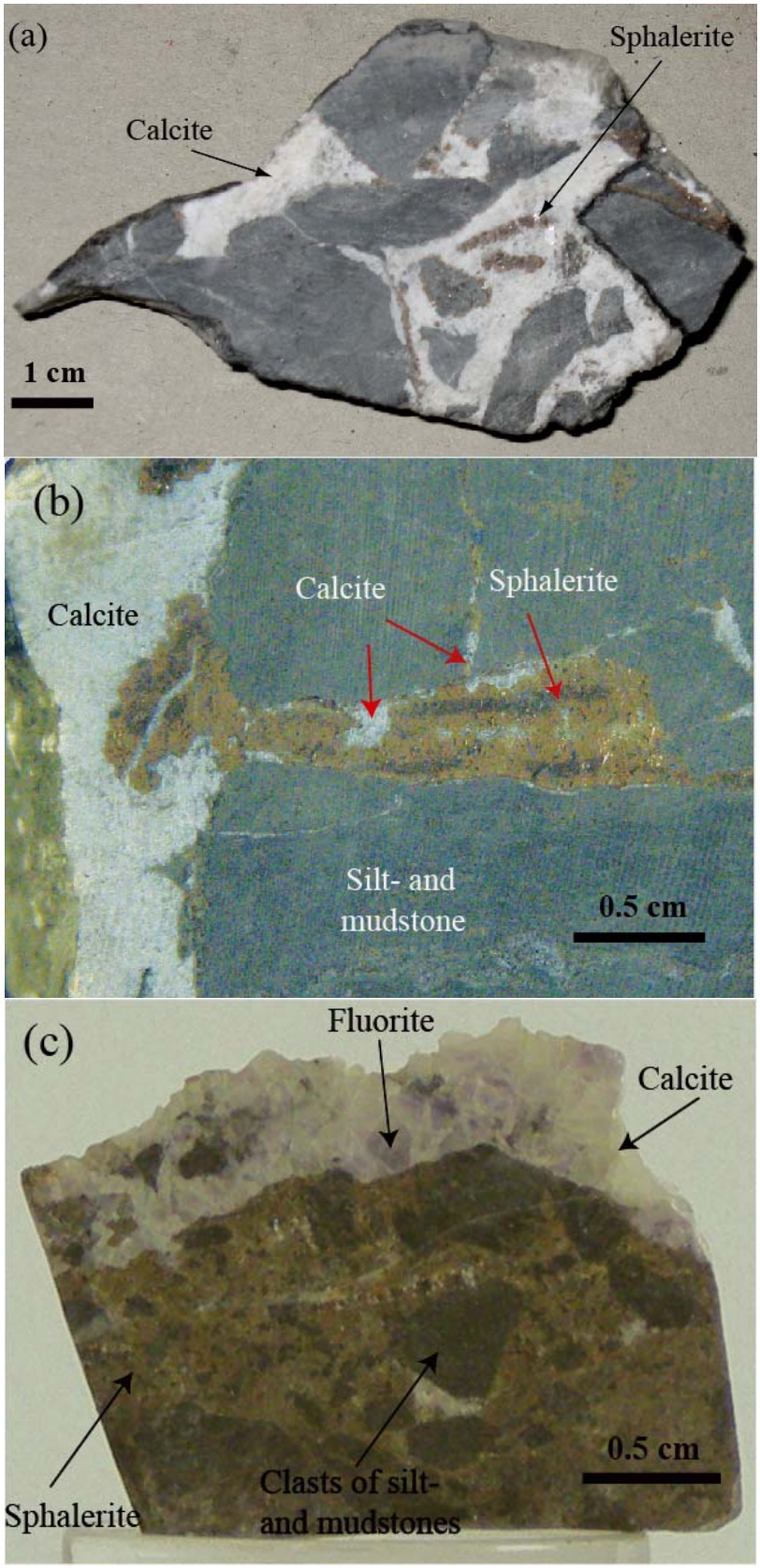

Figure 6. Sphalerite spherulites on the walls of an open fracture at Ersmarksberget.

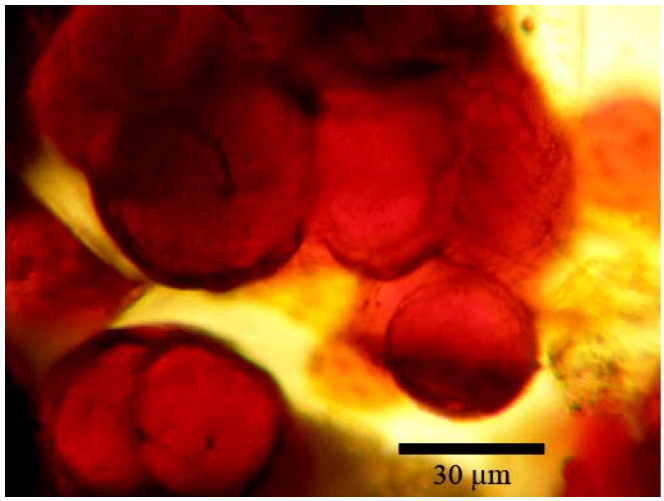

Figure 7. Slightly corroded euhedral pre-mineralisation quartz crystals on the margin of a sphalerite-filled fracture at Svärtträsk.

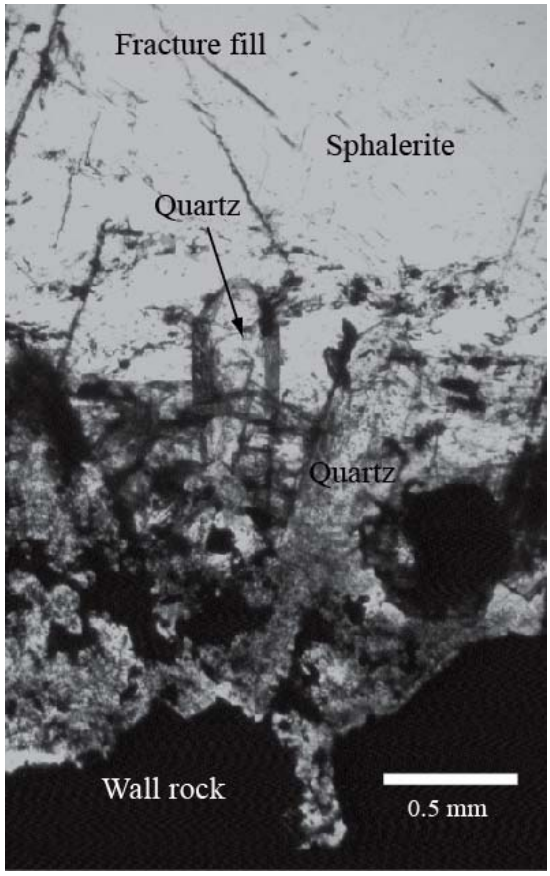

3. Analytical Techniques

Fluid Inclusions

Seventeen drill core samples and hand specimens of veins and breccias were prepared as 150 µm thick doubly polished sections. Fluid inclusions were studied at the Department of Geological

Sciences, Stockholm University by optical microscopy, microthermometry and Raman microspectroscopy. A conventional microscope was used to get an overview and understand the distribution of fluid inclusions. Microthermometric analyses were carried out in the temperature range −196 °C to 600 °C on a Linkam THM 600 heating and cooling stage. The reproducibility is ±0.1 °C for temperatures below +40 °C and ±0.5 °C for temperatures above 40 °C. The stage was calibrated with synthetic fluid inclusion standards (SynFlinc). The calculation of densities for aqueous fluid inclusions utilised the computer program FLUIDS for the H_2O-$CaCl_2$ system [16]. Raman spectroscopic analyses were performed on a multichannel Dilor XY Laser Raman spectrometer. Exciting radiation was provided by the 514.5 nm green line from an Innova 70 argon laser. The laser beam was focused on the sample through a petrographic microscope fitted with a 100× objective and each analysis involved twenty accumulated spectra with a measuring time of 3 seconds. The instrument was calibrated with respect to wave number using a neon lamp and a silicon standard.

Chemical preparation procedures for radiogenic isotope analyses (Sr, Nd, Pb) of rocks and minerals followed standard routines in use at the Laboratory for isotope geology, Swedish Museum of Natural History [17]. Two samples were spiked to allow for a calculation of Rb/Sr ratios (Table 3). A Thermo-Finnigan Triton TIMS instrument was used for the Sr and Nd isotope analyses and data were normalised to $^{88}Sr/^{86}Sr = 0.1194$ and $^{146}Nd/^{144}Nd = 0.7219$. The accuracy of the measurements was monitored by running a series of BCR-1, NBS 987 (Sr), and La Jolla (Nd) standards. The Pb isotope analyses were accomplished by a Micromass IsoProbe multi-collector ICP-MS using an internal Tl tracer to correct for mass bias.

Detailed procedures related to Rb-Sr dating of sphalerite have been described by Schneider [18]. In short, carefully picked, clean separates (10 to 38 milligram) were acid leached, milled thoroughly in a boron carbide mortar to allow a separation of elements (e.g., Rb and Sr) occurring in fluid inclusions from Rb and Sr fixed in mineral lattices. Afterwards, the sample was split into two parts; a leachate and a residual fraction and both were processed through standard ion exchange columns to purify the elements prior to analysis. A Thermo-Finnigan Triton TIMS instrument was used for the Sr isotope analyses, whereas a Finnigan MAT 261 was utilised for Rb.

4. Analytical Results

Fluid inclusion and isotope analyses were carried out on samples of Zn-Pb-mineralised grey to black silty mudrocks and greywackes from the localities mentioned above. Mineralised samples from intrusions were also included.

4.1. Fluid Inclusions

Fluid inclusions hosted in sphalerite, calcite, and fluorite were analysed. Sphalerite is typically zoned from a dark red core, through different shades of orange, to a yellow rim (Figure 8). The calcite is white to light grey and often cloudy, due to a large number of small fluid inclusions. Fluorite is very clear with a violet or green colour. The majority of fluid inclusions are randomly distributed in groups or as individual inclusions, and in places inclusions follow growth planes. Based on their occurrence the inclusions can be classified as primary inclusions. Samples do not display any secondary fluid

inclusions trapped in healed microfractures during a post-mineralisation stage. Moreover, there is no evidence of post-entrapment modifications of the inclusions with changes in volume or leakage.

Figure 8. The upper photo shows a zoned sphalerite crystal from Ersmarksberget. The lower three photos show representative aqueous fluid inclusions in the dark red core, the intermediate orange zone and the yellow margin. The arrow indicates the relative time of deposition and decreasing salinity.

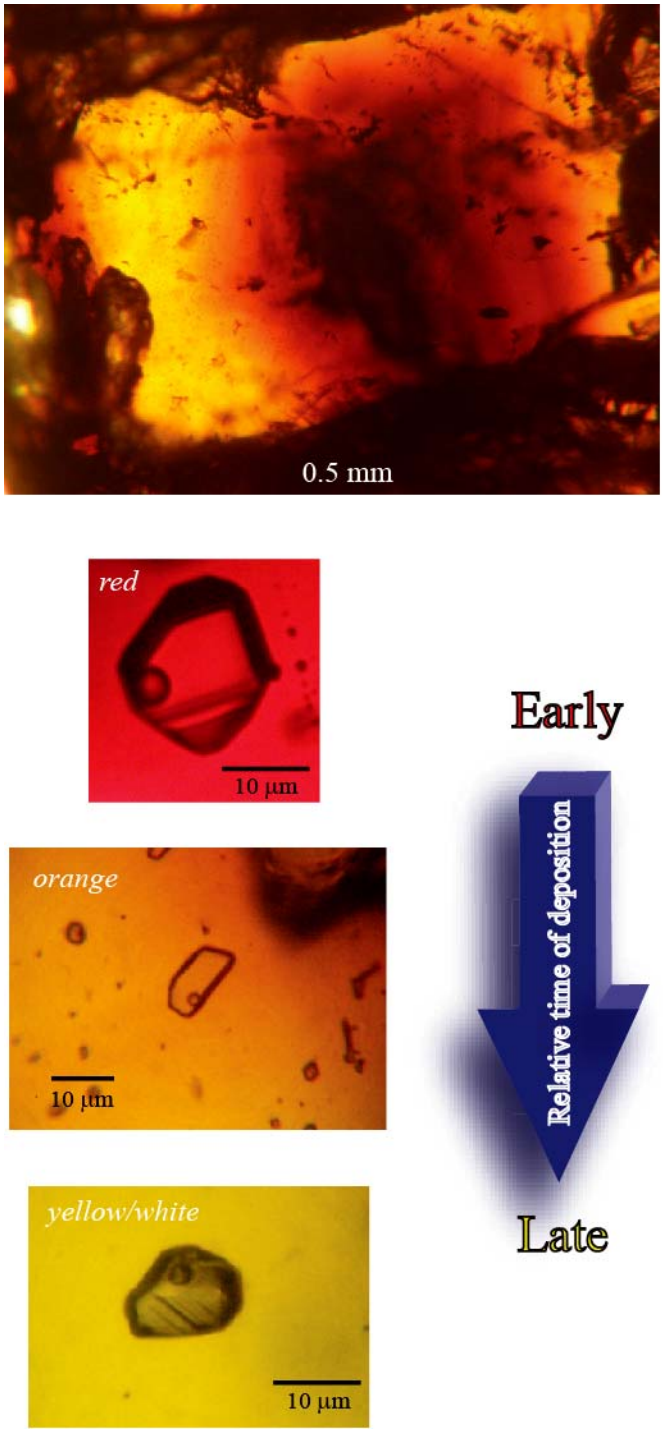

There are two types of fluid inclusions: (i) two phase aqueous inclusions; (ii) hydrocarbon inclusions that coexist with aqueous inclusions in fluorite. The aqueous inclusions comprise a liquid

with a vapour bubble that occupies 2%–5% by volume. In sphalerite (Figure 8), the inclusions can have negative crystal shapes (tetrahedra) or are round or flat. They are up to 60 μm long, but most are less than 10 μm. In calcite (Figure 9), the inclusions have a more or less well-developed negative crystal (rhombohedral) to roundish shape. They are up to 20 μm long, but the majority are <5 μm. Inclusions in fluorite are poorly visible because the refractive index of the liquid is similar to fluorite. The vapour bubbles therefore appear to be free-floating (Figure 10). The inclusions are regular to irregular with a round shape and their size varies from 3 μm to 70 μm.

Figure 9. Photomicrograph of a typical aqueous fluid inclusion in cloudy calcite from Ersmarksberget.

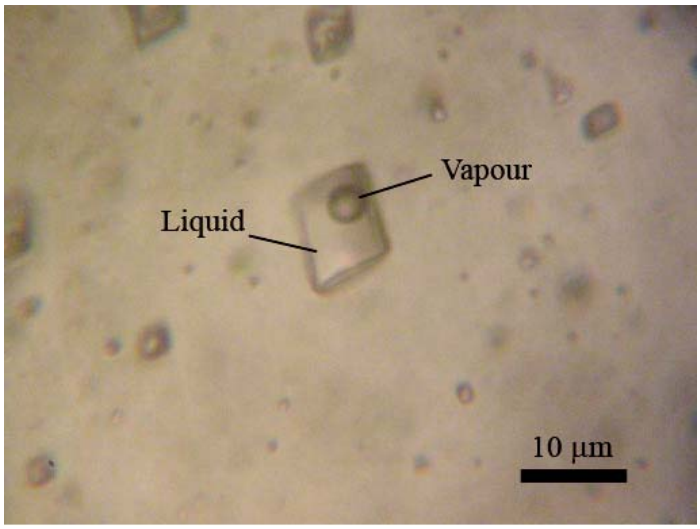

Figure 10. Photomicrograph of fluorite with typical coexisting hydrocarbon and aqueous fluid inclusions from Ersmarksberget. Th = homogenisation temperature, Tm = final ice melting temperature.

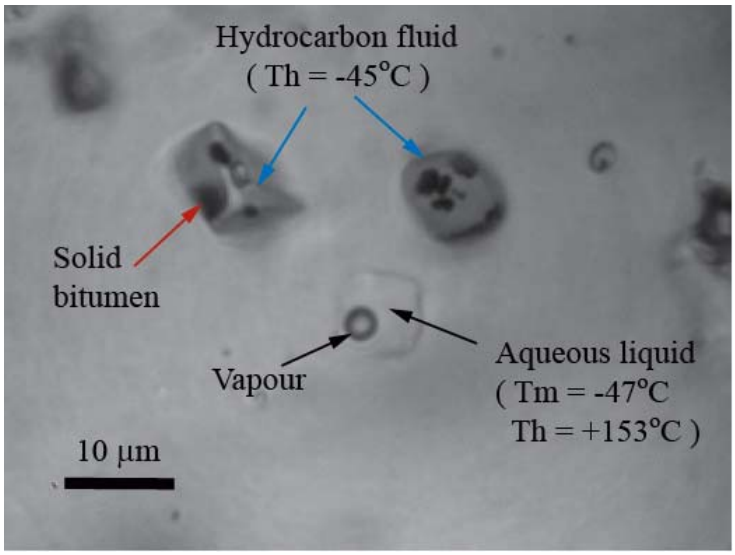

During microthermometry it was difficult to freeze the aqueous fluid inclusions. To achieve total solidification, the inclusions always had to be cooled below −120 °C and then slowly warmed to about

−90 °C when ice became visible. After further heating, initial melting of ice was observed at −70 °C to −60 °C, causing irregular black patches in a fine granular texture in the frozen inclusions. The granular texture gradually became coarser until the final ice melted. Even though it is difficult to interpret phase transitions at such low temperatures unambiguously [19], initial melting or recrystallisation at these low temperatures has been reported for $CaCl_2$-dominated compositions [20]. A $CaCl_2$-rich composition is also the best explanation of the very low final ice melting temperature (see Figure 11).

Figure 11. Frequency histograms of homogenisation and final ice melting temperatures for aqueous fluid inclusions in sphalerite, calcite and fluorite from different Zn-Pb mineralised samples.

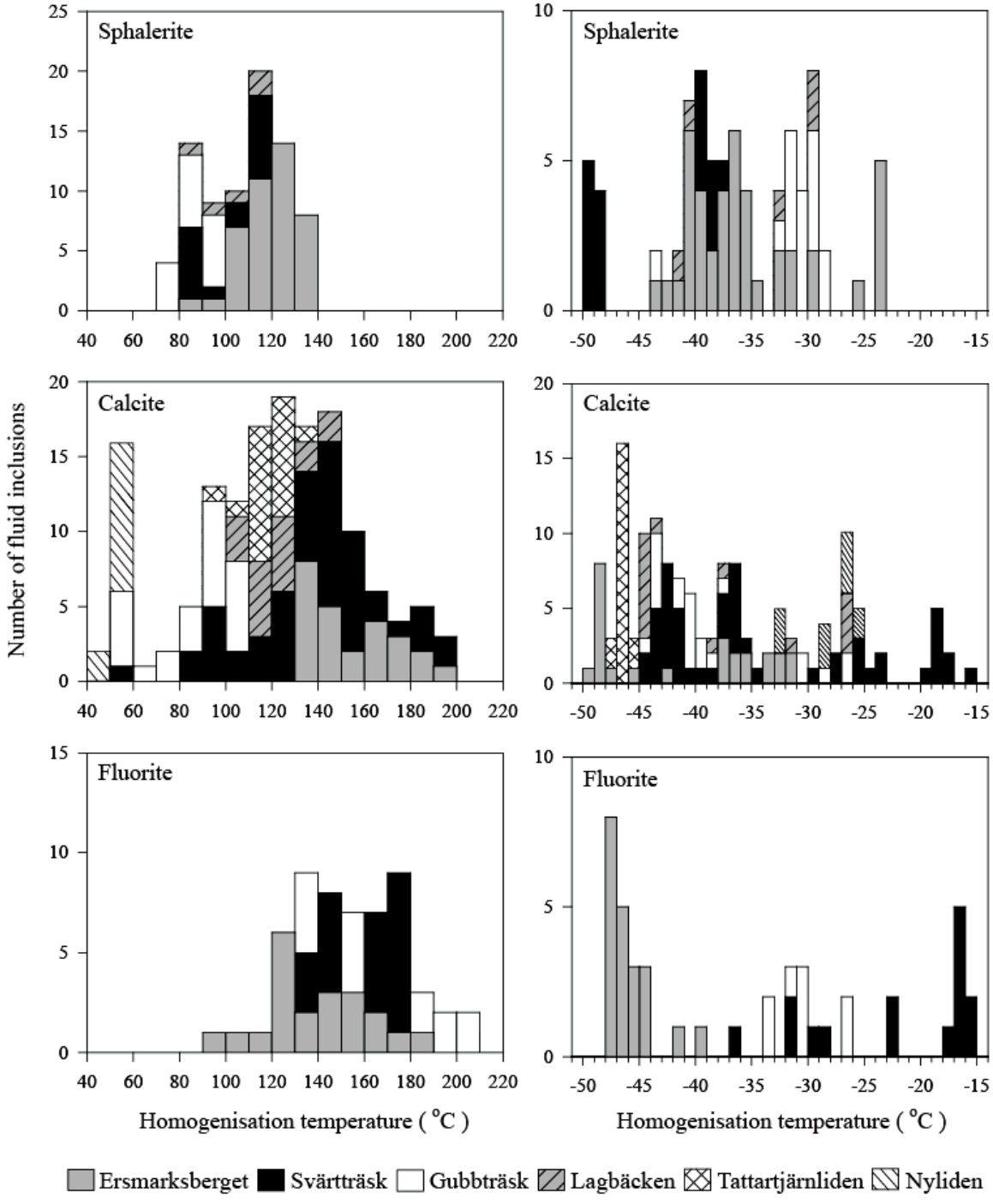

Final ice melting temperature and homogenisation temperatures are presented as histograms in Figure 11 and Table 1. The salinity was determined from the final melting temperature of ice and using the data in [20,21]. In Figure 12 the corresponding salinities are plotted *versus* homogenisation temperatures obtained for all aqueous fluid inclusions. Final ice melting of inclusions in sphalerite occurred at −23.0 °C to −49.0 °C and indicates a salinity of 22.1 to 30.1 eq. mass% $CaCl_2$. A temperature trend was noticed with the lowest melting temperatures obtained for dark red sphalerite and the highest for yellow sphalerite. In calcite, final ice melting was observed at temperatures between −15.9 °C and −49.0 °C, corresponding to a salinity of 18.5 to 30.1 eq. mass% $CaCl_2$. Final ice melting in fluorite occurred between −15.0 °C and −47.6°C, with corresponding salinities of 17.8 to 29.7 eq. mass% $CaCl_2$.

Fluid inclusions in the studied minerals are very sensitive to volume changes during temperature measurements. Overheating may cause stretching (and erroneous homogenisation temperatures) of fluid inclusions. The effect was minimised by heating the inclusions only once. Homogenisation was to the liquid phase in all cases. Homogenisation temperatures of inclusions in sphalerite were measured from 70 °C to 139 °C. There was no divergence in temperature between differently coloured sphalerite. Fluid inclusions hosted by calcite showed the largest span of homogenisation temperatures, from 45 °C to 194 °C. Fluorite displayed homogenisation at temperatures from 96° to 210 °C, with most above 140 °C. The densities for all aqueous fluid inclusions, calculated from homogenisation temperatures, final ice melting temperatures, and using the computer program FLUIDS for the H_2O-$CaCl_2$ system [16], vary between 1.03 and 1.23 g/cm^3.

Table 1. Microthermometric data from aqueous fluid inclusions.

Zn-Pb deposit	**Host mineral**	**n**	**Homogenisation temperature** /°C	**Final ice melting temperature** /°C	**Salinity in eq. mass% $CaCl_2$**
Ersmarksberget	Sphalerite	42	85 to 139	−23.0 to −43.9	22.1 to 28.9
Ersmarksberget	Calcite	25	130 to 194	−31.0 to −49.0	25.1 to 30.1
Ersmarksberget	Fluorite	21	96 to 187	−39.5 to −47.6	27.8 to 29.7
Svärtträsk	Sphalerite	16	83 to 119	−37.8 to −49.0	27.3 to 30.1
Svärtträsk	Calcite	52	59 to 192	−15.9 to −43.0	18.5 to 28.6
Svärtträsk	Fluorite	15	135 to 178	−15.0 to −36.0	17.8 to 26.7
Gubbträsk	Sphalerite	16	70 to 98	−28.3 to −43.8	24.2 to 28.8
Gubbträsk	Calcite	23	50 to 109	−25.8 to −44.0	23.2 to 28.9
Gubbträsk	Fluorite	8	135 to 210	−26.1 to −33.5	23.3 to 26.0
Lagbäcken	Sphalerite	5	83 to 119	−29.0 to −41.0	24.5 to 28.1
Lagbäcken	Calcite	17	104 to 143	−26.0 to −44.0	23.3 to 28.9
Tattartjärnliden	Calcite	20	96 to 133	−45.0 to −47.5	29.1 to 29.7
Nyliden	Calcite	12	45 to 58	−25.9 to −32.9	23.1 to 25.8

Figure 12. Plots of salinity (eq. mass% $CaCl_2$) *versus* homogenisation temperature for aqueous fluid inclusions in (**a**) sphalerite, (**b**) calcite and (**c**) fluorite from different Zn-Pb mineralised samples. The inset box in the sphalerite plot symbolizes the colour-zonation in sphalerite and the decreasing salinity in fluid inclusions hosted by red to yellow sphalerite.

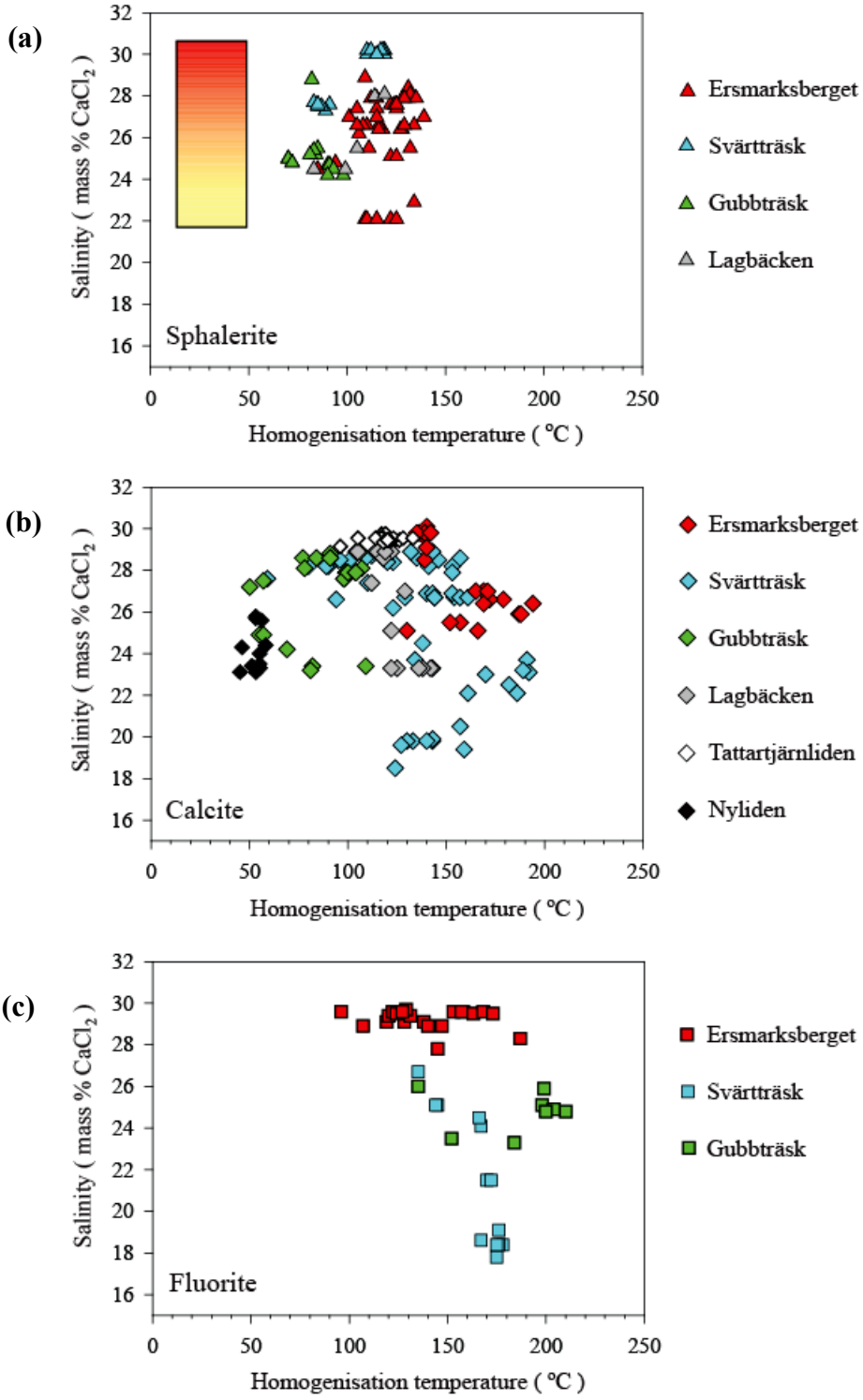

The hydrocarbon fluid inclusions in fluorite consist of a colourless to brownish gas or liquid which frequently contains black bitumen solids (Figure 10). Liquid-filled inclusions occur at random, whereas gas-filled inclusions typically occur in groups close to adjacent calcite. The shape of the

inclusions is round to irregular and they are up to 60 μm. During cooling of the liquid-filled inclusions, a gas bubble appeared and in the gas-filled inclusions a liquid phase emerged. No solid phases were formed. Homogenisation temperatures of the liquid-filled inclusions took place (to liquid) between −41.2° and −55.3 °C (Figure 13). Groups of inclusions filled with the gas phase homogenised (to gas) within a large range of temperatures; for the majority values from −74.9 °C to −77.4 °C were measured, but there were also inclusions where homogenisation occurred at higher temperatures from −30.8 °C to +18.5 °C (Figure 13). Two gas-filled inclusions showed critical homogenisation at −31.0 °C and −79.4 °C respectively. The temperatures are all above the critical temperature (−82.1 °C) of pure methane and suggest that the hydrocarbon inclusions (Figure 13) are composed of a mixture of variable proportions of methane and >1 mole% higher-molecular-weight hydrocarbons [22]. Raman analysis (Figure 14) confirms the presence of methane with a band at 2.911 cm^{-1}, ethane at 2.948 cm^{-1}, propane at 2.892 cm^{-1} [23] and aromatic hydrocarbon compounds at 3.072 [24], and possibly also the weaker band at 3.210 cm^{-1}. The aromatic hydrocarbon compounds include disordered carbonaceous material (bitumen), with Raman bands at 1.340 and 1.604 cm^{-1} [25].

Figure 13. Frequency histogram of homogenisation temperature for hydrocarbon fluid inclusions. T*crit* = critical temperature, indicated by a dashed line. The cross-pattern marks data for brown-coloured inclusions.

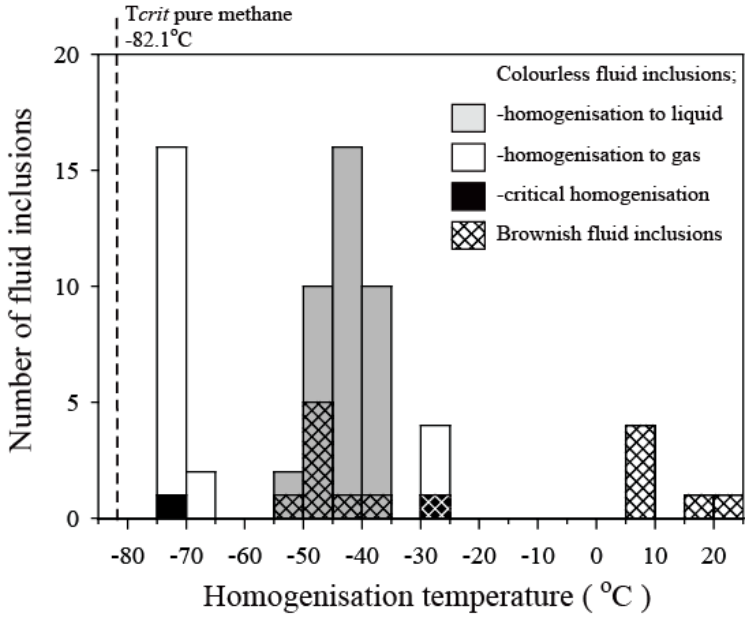

4.2. Pb Isotopes

Pb isotope data were obtained from sphalerite (also analysed for Rb-Sr), galena and gangue minerals from different deposits (Table 2). All show highly radiogenic compositions (Figure 15) with a relatively limited variation. The data form part of a larger trend distinguished by galena data from different deposit types located within, or near the Caledonides [26,27]. It should be emphasised that there is no obvious isotopic difference among different minerals from the same deposit suggesting that Th/Pb and U/Pb ratios (not available) are low for all analysed minerals.

Table 2. Pb data obtained for the residual fraction of treated sphalerite, galena and gangue minerals.

Zn-Pb deposit	Mineral	Sample	$^{206}Pb/^{204}Pb$	$^{207}Pb/^{204}Pb$	$^{208}Pb/^{204}Pb$
Ersmarksberget	Sphalerite	Fa1	23.856	16.284	41.575
Ersmarksberget	Sphalerite	Ea2	23.825	16.273	41.524
Ersmarksberget	Sphalerite	Ea2	23.801	16.278	41.548
Svärtträsk	Sphalerite	Svt 11	23.921	16.306	41.809
Svärtträsk	Sphalerite	Svt 12	23.910	16.305	41.759
Svärtträsk	Sphalerite	Svt 14	23.923	16.298	41.744
Svärtträsk	Sphalerite	Svt 16	23.894	16.288	41.579
Svärtträsk	Sphalerite	Svt 17	23.951	16.303	41.643
Svärtträsk	Sphalerite	Svt 2008	23.886	16.293	41.593
Gubbträsk	Sphalerite	Gut 08, 61.00 m	23.487	16.248	41.51
Gubbträsk	Sphalerite	Gut 18, 93.93 m	24.201	16.333	41.532
Gubbträsk	Sphalerite	Gut 18, 94.04 m	23.513	16.256	41.598
Lagbäcken	Sphalerite	Lab 14, 34.65 m	24.236	16.348	41.808
Ersmarksberget	Galena	97505A, 34.7 m	23.836	16.327	41.827
Ersmarksberget	Galena	97505A, 79.5 m	23.870	16.363	41.939
Ersmarksberget	Galena	97506A, 22.8 m	24.110	16.271	41.207
Ersmarksberget	Galena	97507A, 77.5 m	23.826	16.279	41.703
Gubbträsk	Galena	Gut 18, 94.04 m	23.608	16.266	41.603
Lagbäcken	Galena	Lab 8, 56.80 m	23.947	16.327	41.703
Lagbäcken	Galena	Lab 10, 93.18 m	23.929	16.303	41.746
Tattartjärnliden	Galena	Tfl-185001,65.2 m	24.018	16.321	41.798
Nyliden	Galena	Nyf 21, 198.3 m	22.789	16.157	40.891
Ersmarksberget	Fluorite	Fa1	23.843	16.278	41.558
Ersmarksberget	Fluorite	Ea2	23.891	16.280	41.488
Ersmarksberget	Calcite	Ea2	23.247	16.204	41.087
Gubbträsk	Calcite	Gut 08, 61.00 m	23.406	16.237	41.430
Gubbträsk	Fluorite	Gut 18, 94.04 m	23.645	16.269	41.581
Lagbäcken	Calcite	Lab 08, 56.80 m	23.910	16.304	41.690
Lagbäcken	Calcite	Lab 10, 93.18 m	23.932	16.304	41.688

Figure 14. Laser Raman spectrum of a hydrocarbon inclusion with characteristic bands indicative of the presence of methane, ethane, propane and aromatic components.

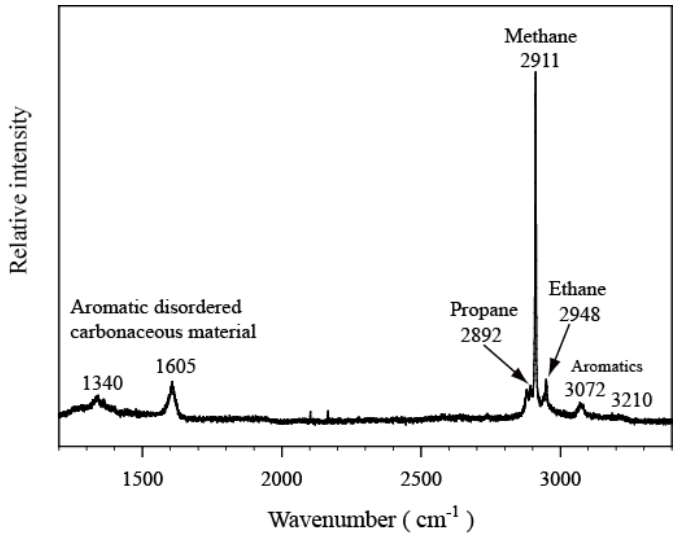

Figure 15. Pb isotope diagram illustrating uniform galena and sphalerite data from fracture-controlled mineralisation types. The data plot on a linear trend defined by clusters of galena from different types of Zn-Pb occurrences. Data sources for different Zn-Pb mineralisation types: fracture-controlled (□ = this study), quartz vein-type (+ = [28]), calcite vein-type (△ = [28]), sandstone impregnation-type (X = [26]). Also added is a field for VMS ores in the Skellefte Ore District (SOD-VMS = [29]), which may approximate the basement lead existing at ca 1.9 Ga, and a reference line which connects the VMS-type of lead with other data.

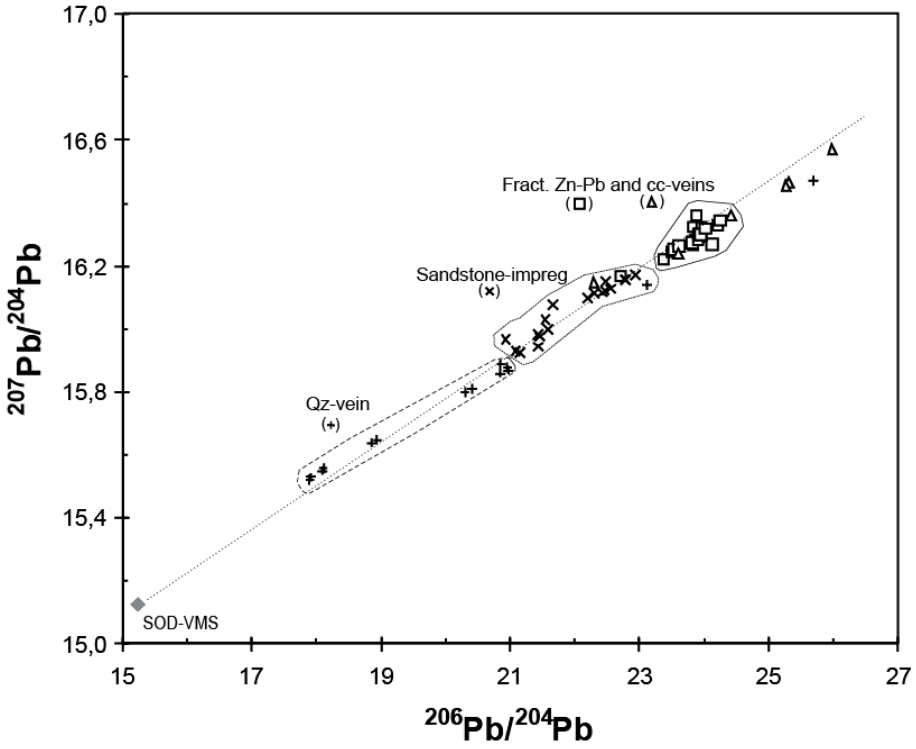

4.3. Rb-Sr Isotopes

Strontium data for Rb-Sr dating were obtained from sphalerites and from gangue minerals (Table 3). For the latter, data are relatively homogeneous with present day $^{87}Sr/^{86}Sr$ ratios between 0.7148 and 0.7198. However, the data from the sphalerite samples is complex (Figure 16). The figure shows analyses of both residuals (R) and leachates (L). There are several unusual features in the residual data: (i) a number of samples show very radiogenic $^{87}Sr/^{86}Sr$ ratios, suggesting unusually high Rb/Sr ratios in their structure; (ii) four sphalerites plot on a straight-line in Figure 16 and, if interpreted as an isochron, its slope indicates a 531 ± 21 Ma (MSWD = 2.4) age. There are problems, however, reproducing the data because of the complex isotopic nature of the sphalerite systems (see discussion), which also implies that quoted MSWD values (the assigned 2 sigma relative errors are 0.3% and 0.1% in the Rb/Sr and Sr ratios, respectively), are not a robust indicator of the isochron quality; (iii) those samples that do not fit the *ca.* 530 Ma "isochron" appear to plot randomly in Figure 16. The leachates (L) have comparatively low Rb contents, but their $^{87}Sr/^{86}Sr$ ratios vary considerably with some of these samples plotting relatively near the data cluster defined by the gangue phases.

Figure 16. Rb-Sr data for the sphalerite samples used for dating the fracture-controlled Zn-Pb deposits. Also shown are data for gangue minerals.

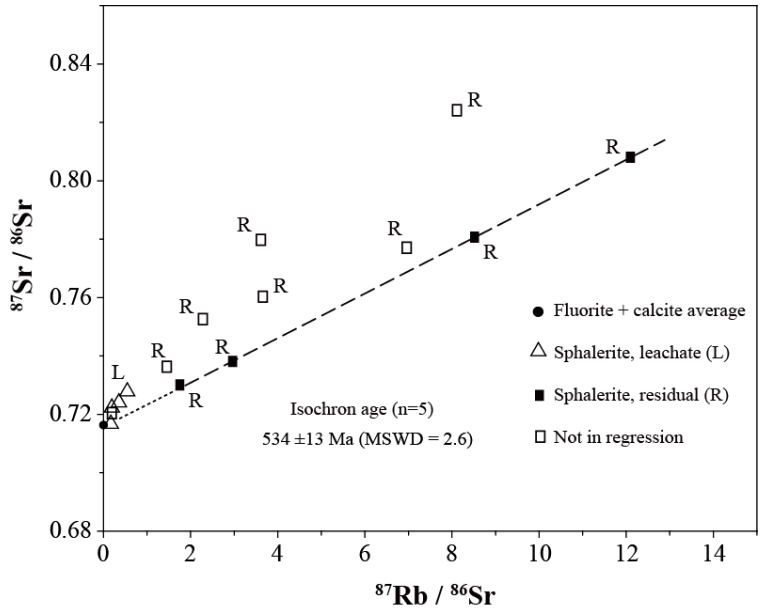

Table 3. Rb-Sr data of sphalerite samples, separated into a residual (R) and a leachate (L) fraction. Also included are two gangue minerals from Ersmarksberget.

Zn-Pb deposit	Sample [1]	Fraction	Rb/ppm	Sr/ppm	$^{87}Sr/^{86}Sr$	$^{87}Rb/^{86}Sr$
Ersmarksberget	Fa 1	R	0.756	0.317	0.77743	6.9519
Ersmarksberget	Fa 1	L	0.534	4.493	0.72480	0.3446
Ersmarksberget	Ea 2 h	R	0.507	0.174	0.78086	8.5005
Ersmarksberget	Ea 2 db	R	0.103	0.101	0.73842	2.9673
Ersmarksberget	Ea 2 db	L	0.026	0.747	0.71597	0.1021
Svärtträsk	Svt 11	L	0.174	2.752	0.72280	0.1830
Svärtträsk	Svt 12	R	0.085	0.141	0.73031	1.7466
Svärtträsk	Svt 14	R	0.092	0.073	0.76046	3.6685
Svärtträsk	Svt 14	L	0.094	1.601	0.71740	0.1697
Svärtträsk	Svt 16	R	0.191	0.155	0.77987	3.5965
Svärtträsk	Svt 16	L	0.061	0.330	0.72825	0.5374
Svärtträsk	Svt 17 [2]	R	0.301	0.109	0.82426	8.1097
Svärtträsk	Svt 17	L	0.077	0.821	0.72492	0.2708
Svärtträsk	Svt 17A db	R	0.013	0.183	0.72102	0.2122
Svärtträsk	Svt 17A	L	0.051	1.246	0.72046	0.1196
Svärtträsk	Svt-02-08	R	0.010	0.133	0.72108	0.2136
Svärtträsk	Svt-02-08	L	0.104	2.194	0.72092	0.1378
Gubbträsk	Gut 08, 61.00	R	0.612	0.148	0.80804	12.070
Gubbträsk	Gut 08, 61.00	L	1.104	2.299	0.73344	1.393
Gubbträsk	Gut 18, 93.93	R	0.031	0.062	0.73686	1.441
Gubbträsk	Gut 18, 93.93	L	0.025	0.676	0.71702	0.109
Gubbträsk	Gut 18, 94.04	L	0.173	1.313	0.73027	0.383
Lagbäcken	Lab 14, 34.65	R	0.149	0.182	0.75155	2.379

Table 3. *Cont.*

Zn-Pb deposit	Sample 1	Fraction	Rb/ppm	Sr/ppm	$^{87}Sr/^{86}Sr$	$^{87}Rb/^{86}Sr$
Ersmarksberget	Ea2, calcite	gangue	0.203	120.3	0.71488	0.0049
Ersmarksberget	Ea2, fluorite	gangue	0.097	15.92	0.71745	0.0177

Note: 1. analysed sphalerites are brown-coloured; a few have a more distinct honey (h) or dark-brown (db) colour; 2. two specimens were independently separated from sample Svt17.

4.4. Nd Isotopes

Seven Nd istope analyses of gangue minerals from three different deposits yielded a range in $^{143}Nd/^{144}Nd$ ratios between 0.51146 and 0.51183 (Table 4). When plotted on the Sm-Nd isochron diagram (Figure 17) certain variations in initial $^{143}Nd/^{144}Nd$ ratios are indicated between mineralised samples, and there are also within-deposit variations indicated for Ersmarksberget samples. The data scatter, also noted for the Sr isotope ratios of corresponding samples, and the possibility that calcite, which may be easily affected by post-crystallisation events, has not remained a closed Sm-Nd isotope system preclude a reliable estimate of formation age(s). ε-Nd values calculated for two tentative formation ages yield similar ranges between −14.0 and −18.5 (530 Ma, from Rb-Sr data), and −15.0 and −18.4 (400 Ma, Caledonian age), respectively. T-DM ages [30] are in the range 1.8–3.5 Ga (Table 4).

Table 4. Sr and Nd data for gangue minerals.

Zn-Pb deposit	Sample	Mineral	Sm /ppm	Nd /ppm	$^{143}Nd/^{144}Nd$	$^{147}Sm/^{144}Nd$	Nd 0 Ma	t-DM (91)[1]	□□Nd 400 Ma	□□Nd 530 Ma	$^{87}Sr/^{86}Sr$
Ersmarks-berget	Fa1	Fluorite	1.7	7.4	0.511573 ± 15	0.1385	−20.8	3.13	−17.6	−16.9	0.71985 ± 10
Ersmarks-berget	Ea2	Fluorite	1.8	7.3	0.511679 ± 4	0.1511	−18.7	3.51	−16.3	−15.6	0.71628 ± 05
Ersmarks-berget	Ea2	Calcite	19.7	96.3	0.511629 ± 5	0.1235	−19.7	2.50	−15.7	−14.7	0.71563 ± 02
Gubbträsk	Gut 08, 61.00m	Calcite	33.2	186.1	0.511463 ± 4	0.1077	−22.9	2.37	−18.1	−16.9	0.71511 ± 06
Gubbträsk	Gut 18, 94.04m	Fluorite	92.1	275.5	0.511710 ± 5	0.2021	−18.1		−18.4	−18.5	0.71483±04
Lagbäcken	Lab 08 86.80m	Calcite	48.7	151.0	0.511827 ± 5	0.1949	−15.8		−15.8	−15.7	0.71365 ± 03
Lagbäcken	Lab 10, 93.18m	Calcite	85.0	419.0	0.511666 ± 5	0.1226	−19.0	1.80	−15.0	−14.0	0.71446 ± 01
Tattar-tjärnliden	Tfl-1 85001, 65.2m	Calcite									0.71544 ± 02

Note: 1. Depleted mantle model ages were calculated according to De Paolo *et al*. [30].

5. Discussion

Our work demonstrates that the geology of all studied Zn-Pb deposits in the area is similar. Ore occurs in brittle structures that cut Early Proterozoic mudrocks, greywackes, and to a lesser extent, volcanic and intrusive rocks. The fracture-controlled ore minerals occur in veins and breccias that strike NE to N. These cut Svecofennian structures and schistosity. There is also evidence, such as brecciated ore, of minor reactivation of faults. Sphalerite and galena dominate, with subordinate fluorite, calcite and local quartz. Wall-rock alteration is virtually absent. Fluid inclusion data indicate a range of salinities between 18 and 30 eq. wt% $CaCl_2$ and temperatures from 45 °C to 210 °C. Pb isotope data are relatively uniform and highly radiogenic. The similarities between the areas suggest a common epithermal-style ore-forming event that took place during a geologically short period. On the basis of cross-cutting relationships, this must post-date the 1.8 Ga Svecofennian schistosity. Potentially, ore deposition may have coincided with the one of the following events: (i) 1.2–1.1 Ga rifting and related doleritic magmatism [31]; (ii) pre-Caledonian, ≥0.6–0.5 Ga rifting during opening of the Iapetus; (iii) 0.5–0.4 Ga Caledonian orogeny; (iv) 0.3 Ga rifting, locally known from the Oslo region [32]. However, no unequivocal radiometric age evidence constraining ore formation has been published, and although lead isotope data for galena in Zn-Pb veins seem to rule out a Grenvillian origin [26] such data cannot be used to separate events in the 0.6–0.3 Ga time interval. Following this, the available analytical data and other evidence are used below to focus on the two most likely genetic models; a pre-Caledonian (Cambrian) rifting origin *versus* a Caledonian (Silurian) thrusting scenario.

Figure 17. Sm-Nd diagram showing data for gangue minerals (full sample numbers are given in Table 4) from three fracture-controlled Zn-Pb deposits. The reference line is drawn to include all seven points.

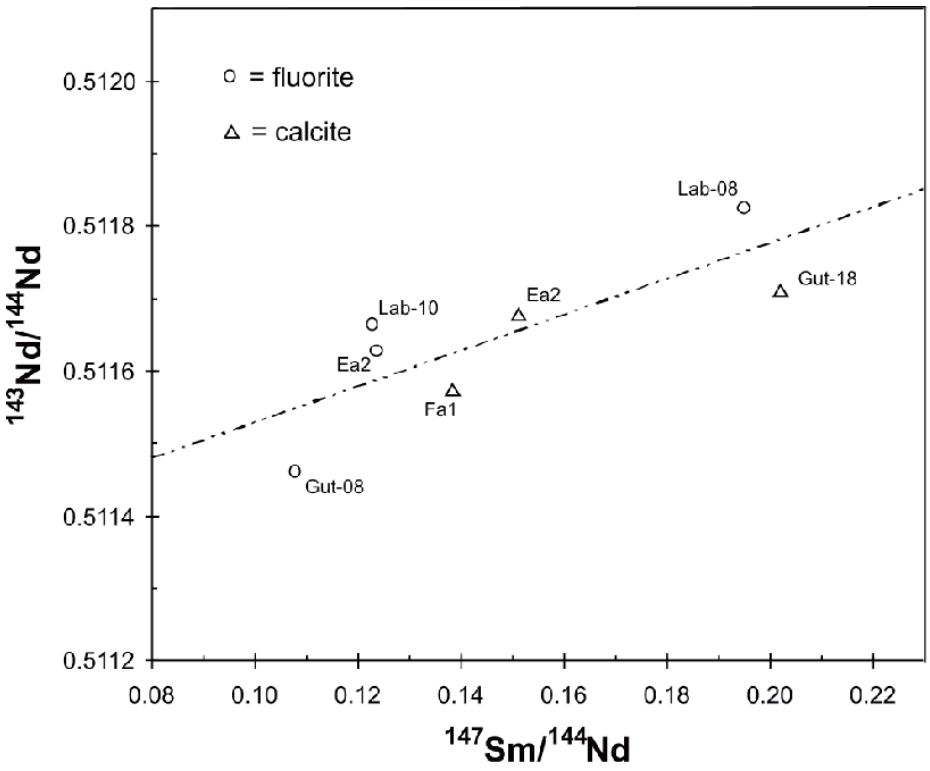

5.1. Constraints from Fluid Inclusions

Fluid inclusion data show that the six Zn-Pb occurrences formed from aqueous fluids of similar composition and temperature with minor deviations. Homogenisation temperatures of all aqueous inclusions in sphalerite, calcite and fluorite indicate deposition at low-temperature conditions, below 200 °C. The data indicate early sphalerite formation, around 100 °C (±30 °C), followed by calcite at increasing temperature to about 200 °C, and finally fluorite growth during subsequent cooling. The mineralising fluid was rich in $CaCl_2$ with a salinity of 18 to 30 eq. mass% $CaCl_2$. The salinity and homogenisation temperatures (Figure 12) are typical of MVT deposits [33].

There is no clear relationship between homogenisation temperatures and salinities, but one probable interpretation is fracture-controlled mixing between a relatively warm (~200 °C) brine with a salinity of about 18 eq. mass% $CaCl_2$ and a cooler (<70 °C) sedimentary brine with a salinity of 30 eq. mass% $CaCl_2$. The variation in homogenisation temperature seen especially in data from calcite and fluorite is not a typical mixing trend, but could be explained by mixing combined with different degrees of cooling, or heating, during migration in the fractures or alternatively mixing between different proportions of the two brines. In addition, the colour zoning noted for sphalerite in the LSOD is best explained by variable mixing proportions between two fluids of contrasting chemical and isotopic properties, whereby the growth of sphalerite (from red to yellow) is related to successively increasing amounts of mixing of a distal fluid in fractures where a local fluid was already present.

In an inferred mixing model, Zn and Pb were transported by the warmer fluid as chloride complexes. Anoxic conditions prevailed during mixing with the cooler fluid, carrying reduced sulphur, in open spaces (fractures) leading to the precipitation of sphalerite and galena. Simultaneous calcite and sphalerite growth points to a slightly alkaline pH. High pH is also supported by corroded early quartz crystals in some of the sphalerite-filled cavities (Figure 7). Zoned sphalerite demonstrates an evolution, with gradually decreasing salinity. Early dark red (Fe-rich) sphalerite showed the highest values (close to 30 eq. mass% $CaCl_2$). Later yellow sphalerite had the lowest salinity (close to 20 eq. mass% $CaCl_2$) (Figure 12). Secondary fluid inclusions are absent, indicating no significant post-mineralisation processes.

Aqueous fluid inclusions are all two-phase; they show no evidence of boiling at the time of trapping and have constant liquid to vapour ratios. The homogenisation temperatures are therefore probably minimum trapping temperatures. Furthermore, the presence of higher-molecular-weight hydrocarbons in the inclusions implies that it is unlikely that the temperature exceeded ~200 °C [25]. At higher temperatures the hydrocarbon compounds would have evolved to methane. The large variation in homogenisation temperatures, with homogenisation both to liquid and gas, critical homogenisation at different temperatures, and coloured and uncoloured hydrocarbons (Figure 13), indicate variable hydrocarbon compositions. This difference may reflect different degrees of heating due to fluctuations in temperature during fluorite growth.

Some inclusions contain hydrocarbons with less degradation, whilst others are more evolved. In our model, hydrocarbons were generated by heating of organic matter in the Middle Cambrian autochthonous organic-rich Alum Shale. Coexisting hydrocarbon and aqueous fluid inclusions (Figure 10) suggests that hydrocarbons were involved in mineralisation. A genetic link between hydrocarbons and mineralising fluids has often been proposed for MVT deposits [34] and references therein]. Besides

creating an anoxic environment, the hydrocarbons may have provided reduced sulphur for sulphide deposition by the release of organically bound sulphur or by thermochemical reduction of sulphate from evaporate rock or seawater [35].

5.2. Pb-Pb data of Ore Minerals and Associated Gangue Phases

Lead isotope analyses for sphalerite, galena, calcite and fluorite yield highly radiogenic compositions (Figure 15) with relatively small isotopic differences between phases. Textural relationships indicate that calcite and fluorite formed after galena and sphalerite, and, given the common fluid inclusion characteristics, this happened as part of the same event. Importantly, there is essentially no difference in lead isotopic compositions for the different minerals within each deposit, suggesting a common Pb source for all deposits.

Our Pb-Pb data form part of a larger, more regional scale, linear array (Figure 15) that includes sulphide-bearing calcite veins, quartz veins, and sandstone-impregnation type mineralisation from, or near, the Caledonides [26]. Johansson and Rickard [26] discussed the significance of radiogenic Phanerozoic ore Pb and suggested a two-stage model whereby Pb derived from the 1.8 ± 0.15 Ga Svecofennian basement became involved in ore formation at 0.4 ± 0.15 Ga. The relatively large error in the age(s) of the Pb mobilisation (galena-forming) event is due to uncertainties in the slopes of linear arrays, and possible initial isotopic heterogeneities of the bedrock supplying the Pb component. Therefore, available Pb isotope data do not allow a distinction between galena forming stages that are closely related in time, for instance at e.g., ~530 Ma (an event discussed in this study) or ~420 Ma (Caledonian peak-metamorphic event).

The current isotope data from the fracture-controlled deposits place some additional constraints on the source of Pb. Based on fluid inclusion evidence and microscopic work, it is likely that ore and gangue formed by mixing of two brines. The observed Pb isotope homogeneity suggests that Pb was largely supplied from one of these fluids. Further, given the diversity in host rocks, it is reasonable that the Pb component was derived from a distal and quite homogenous source. The isotopic homogeneity also implies that selective leaching is unlikely as it would produce more heterogeneous data. Instead, leaching of a total rock lead component is envisaged. Considering that 1.80 ± 0.02 Ga Revsund granites, which have great vertical extent [36], dominate the LSOD, this rock is a potential source of Pb. This view is strengthened by preliminary whole rock Pb data for Revsund granites (Billström, unpublished results), which, when back-calculated to 500 Ma, overlap with the observed Pb ore data range. The low Pb isotope ratios of pre-1.8 Ga sedimentary and volcanic rocks indicate that these lithologies are not potential contributors. Nor can sediments containing erosional material from the Skellefte VHMS deposits have been important, because they carry non-radiogenic lead ($^{206}Pb/^{204}Pb$ is around 15.2 for most deposits [29].

5.3. Sr-Nd Isotope Data of Gangue Minerals

Although sphalerite and gangue formed during the same event, the inferred initial Sr isotope compositions for most of the sphalerites are clearly different to that of the Ca-rich gangue minerals. Based on the generally low Rb/Sr ratios, inferred for the gangue minerals (Table 3), the relatively

small variation found in their measured $^{87}Sr/^{86}Sr$ isotope ratios (*ca.* 0.715 to 0.720) probably reflects the situation at crystallisation.

As described earlier, it is impossible to calculate Sm-Nd dates. The Nd source in the gangue minerals can be better understood using approximate initial Nd isotope ratios which, when calculated for two Phanerozoic ages, indicate relatively uniform values in the range −14 to −18 (Table 4). These Nd isotope ratios are strongly negative and the variation is quite small between the Zn-Pb localities despite their different host rocks. This suggests a fairly homogeneous single, regionally available source with only minor influence from other sources. A dominant Proterozoic component, which had evolved at ~0.5 Ga to strongly negative compositions could explain this isotopic range. The estimated ε-Nd isotope ratio in the Iapetus Ocean was −2.7 to −5.4 [37], and even if seawater-derived fluids were involved in ore formation, the very low REE concentrations in seawater imply that it had almost no effect on the Nd isotope signature in gangue minerals. Depleted mantle Nd model ages [30] vary between 1.80 and 3.51 Ga, and are thus also compatible with a dominant Proterozoic Nd component(s) in the ore-forming solutions. Consistent with Pb isotope systematics, this supports a leaching model with Nd supplied mainly by basement rocks.

5.4. Rb-Sr Data for Sphalerite

Rb-Sr data for sphalerite are complex to interpret and the following discussion aims to shed light on the isotopic nature of two inferred end-member fluids and the significance of the observed linear Rb-Sr isotope array.

5.4.1. Scattered Rb-Sr Data—A Result of a Mixing Process Involving Two Fluids

The range in measured $^{87}Sr/^{86}Sr$ ratios is very large and the decay of ^{87}Rb to ^{87}Sr during the relatively short time that has passed since ore formation (≥0.5 or ≥0.4 Ga, dependent on the preferred model) can only account for a very small part of the scatter. Besides, as the ores are seemingly unaffected by any significant post-mineralisation process that could have affected the Rb-Sr systematics, there must have been a very large isotopic contrast developed at the time of ore formation. This suggests that Sr in the ores was supplied from two sources; an old source (with strongly radiogenic Sr isotope signatures) and a young source (featuring a common Sr component). One possibility is that the isotope scatter is caused by fluid-rock interaction processes, whereby a single-sourced fluid incorporates Sr both from the old basement (radiogenic component) and seawater. Although this may provide a reasonable explanation for the relatively minor variability in Pb isotope data, it is unlikely that one specific ore fluid can produce the mixed radiogenic-unradiogenic Sr isotope compositions that are observed on a sampling scale. A fluid mixing model is preferred to explain the isotope patterns, and the variations in temperature and salinity. Such a model has also been suggested for other deposits sharing similar fluid inclusion evidence; e.g., the calcite vein deposits studied by Johansson [38] and the sandstone-impregnated type [3].

5.4.2. The Radiogenic End-member Fluid

Several sphalerite samples (Figure 16) indicate a considerable scatter in initial Sr isotope signatures which suggests the presence of a radiogenic fluid. If the sphalerites formed during one short event, and there were no secondary disturbances of Rb-Sr systems (as suggested by fluid inclusions), then each sample acted as a closed system since crystallisation. Present-day Sr isotope ratios of sphalerites are therefore controlled by their respective initial Sr isotope ratio and $^{87}Rb/^{86}Sr$ ratios, implying that the observed Rb-Sr data scatter is a direct measure of the variability for the initial Sr incorporated in sphalerite. By constructing hypothetical 530 Ma reference lines (not shown on Figure 16) drawn through each individual data point, the different intercepts with the y-axis indicate that the initial Sr ratio in sphalerites varied from *ca.* 0.715 to *ca.* 0.760. Thus, the Sr in a radiogenic fluid (referred to as the *hot fluid*) was characterised by a $^{87}Sr/^{86}Sr$ ratio of 0.760 or higher. We suggest that this fluid carried Sr from the early Proterozoic basement. Based on previously published Rb-Sr data of granitoids forming the basement in the study areas [39], the bulk of $^{87}Sr/^{86}Sr$ present-day ratios are between 0.76 and 0.78 (between 0.75 and 0.77 when back-calculated to 530 Ma). Such basement data are radiogenic enough to be compatible with the inferred radiogenic Sr source (which dominates the hot fluid) at the time of ore formation.

5.4.3. The Non-Radiogenic End-Member Fluid

At first glance, the sphalerite data in the Rb-Sr isochron diagram (Figure 16) are apparently random. However, this is exactly the pattern expected if two solutions are mixed at the site of sphalerite precipitation, implying that different samples are likely to crystallise with variable Sr isotope compositions. Nevertheless, given the apparent linear array defined by some of the data, a straight-line has been drawn through four points representing residual sphalerites (see Figure 16). To understand if this line has any geological significance, three different options are considered; the linear array is either a mixing line, or a rotated isochron, or a valid isochron. A mixing hypothesis can be tested by plotting the measured Sr isotope compositions of the four samples *versus* 1/Sr concentration. However, the randomness in such a plot (not shown) argues against a mixing process. The possibility of the linear array reflecting a rotated isochron implies resetting of the isotope systematics during a post-depositional event. In such a case, the calculated age reflects a secondary event and the true sphalerite formation age must be older than *ca.* 530 Ma. Geological data and temporal constraints, see below, do not favour the possibility of an ore-forming event occurring before the start of the Cambrian period. The remaining hypothesis is that the 4-point linear array corresponds to a "true" Rb-Sr isochron, and in the following paragraphs this possibility is further explored.

If a mixing model, involving fluids carrying isotopically different components is relevant, the only way of producing an "isochron" is to assume that certain samples obtained their elements from a single fluid, or from a mixed fluid that was homogeneised or totally dominated by one fluid source. Other restrictions are that samples must have a common age and show no signs of a post-crystallisation disturbance affecting the Rb-Sr isotope systematics. There are several observations indicating that these criteria are fulfilled (Figure 16): (i) available calcite and fluorite samples from three mineralised samples indicate similar $^{87}Sr/^{86}Sr$ isotope ratios (0.715 to 0.720) suggesting the presence of a

regionally available, important end-member fluid with a narrow isotopic composition; (ii) the four-point sphalerite "isochron", based on residual data, indicates an initial Sr isotope composition of 0.7158 that is comparable with the above outlined end-member fluid and this provides evidence against the view that linearity is simply coincidental; (iii) there are no sphalerites among the scattered population plotting below the tentative "isochron", which reinforces the notion that all samples on the "isochron" had initial Sr isotope compositions that approximate that of the low-radiogenic (~0.716) fluid end-member; (iv) Rb-Sr data from leachates reflect the isotopic composition of the water component in fluid inclusions. In this case, where fluid inclusions are in chemical equilibrium with their hosts and there are no secondary inclusions, such data provide a direct link to the isotopic nature of local ore fluids. The least radiogenic leachate (*i.e.*, Ea2 db, which is a sample for which the connected residual sample plots on the "isochron") is characterised by a low Rb/Sr ratio (Table 3) and the measured Sr isotope composition (0.71597) is therefore close to its initial Sr isotope signature calculated to around 0.7152 (at 0.5 Ga). This value is practically identical to the initial value given by the 4-point sphalerite regression, a similarity supporting the geological relevance of the inferred "isochron"; (v) fluid inclusion evidence suggests that no post-crystallisation processes affected the Rb-Sr system; (vi) the Zn-Pb fracture-controlled vein ore type is unique and only occurs in the area east of the Caledonian margin and is probably the result of a single ore-forming episode. It is therefore plausible that this ore-forming event took place during a geologically short period, and given the analytical errors involved in the Rb-Sr age estimate the mineralised rocks studied can be assumed to share a common emplacement age.

The observation that the initial Sr isotope ratio for the tentative four-point sphalerite isochron (*ca.* 0.716) is close to data from the suite of Ca-rich gangue minerals has further implications. That latter carry the bulk of Sr in the ore systems, and these minerals have very low $^{87}Rb/^{86}Sr$ ratios (Table 3), which means that the effect of in-situ decay of ^{87}Rb to ^{87}Sr is marginal; the difference between measured and back-calculated (534 Ma) $^{87}Sr/^{86}Sr$ ratios lies in the fourth or fifth decimal. This suggests that the original Sr isotope compositions of gangue phases, developed at the time of crystallisation, are well approximated by their measured Sr isotope ratios. Keeping this in mind a fifth point, representing the gangue minerals has been included in an alternative regression. By using the average $^{87}Sr/^{86}Sr$ value of 0.7157 for calcite and fluorite data from those sample sites (Ea2 and Gut-08, 61.00 min Table 3) from which the previous regression was based, this results in an age of 534 ± 13 Ma (MSDW = 2.6).

Altogether, even if the method used is not particularly robust, it is suggested that the included sphalerites, and gangue minerals, were deposited from an isotopically distinct fluid and can be used to derive the 534 Ma "isochron". The indicated ore formation age and the palaeogeography at the time suggest that marine (Iapetus Ocean), early Cambrian Sr ($^{87}Sr/^{86}Sr$ ratios close to 0.709) may be one part of the fluid that deposited the gangue. However, another, more radiogenic, source is required to explain the gangue Sr isotope signature close to 0.716. This may indicate that seawater mixed with surface water that had interacted with sedimentary rocks composed of eroded Late Precambrian rocks, which contributed some radiogenic ^{87}Sr. We propose that when such a fluid (referred to as the *cool fluid*) approached the site(s) of ore deposition it had a quite homogeneous $^{87}Sr/^{86}Sr$ signature close to 0.716. If the overall scenario is valid, the Sr isotope pattern of sphalerite (Figure 16) illustrates the behavior of two populations of fluids; a scattered population of samples (carrying a mixture of Sr from

the hot and cool fluid) plus a low-radiogenic population characterised by a common initial Sr component (corresponding to Sr contributed solely from the cool fluid).

5.5. A Comparison between the LSOD Zn-Pb Deposits and Nearby Sulphide Occurrences

The LSOD Zn-Pb deposits represent a distinct sulphide ore type, at some distance from the present Caledonian margin. Besides the studied deposits, similar basement-hosted occurrences, of less economic importance, have been reported from the area. Johansson [38] briefly described sulphide-bearing calcite veins at Åkerlandet (30 km south of the map area in Figure 1) and Juktnäs (Figure 2). These calcite veins tend to occur in an approximately N- to NE-direction and are dominated by calcite gangue with lesser amounts of fluorite, sphalerite, galena and pyrite. The sphalerite is zoned as demonstrated by Åkerlandet [40]. A radiogenic Pb component is present and Pb isotope data from Åkerlandet and Juktnäs [28] overlap data from this study. Fluid inclusions from Åkerlandet indicate mineralisation temperatures between 80 °C and 170 °C, and a depositional event involving two saline fluids [28]. This is consistent with our data from the fracture-controlled Zn-Pb deposits and we consider the Juktnäs and Åkerlandet deposits to be analogous to those investigated in the present study.

Other 0.4–0.6 Ga sulphide ore types within the Caledonides and along its margin include: (i) stratiform base metal ores in the higher Caledonian nappes [41] and references therein; (ii) caledonian sulphide-bearing quartz veins [27,28]; (iii) sandstone hosted Zn-Pb impregnation ores at the margin [2,42]. The stratiform ore type comprises polymetallic chalcopyrite-rich massive sulphide deposits that have been affected by high-temperature (≥400 °C) Caledonian metamorphism and deformation [43]. The Pb isotope composition is much less radiogenic than the fracture-controlled Zn-Pb deposits in the Storuman area [44].

Caledonian sulphide-bearing quartz veins occur within the interior parts of the Swedish Caledonides, in tectonic positions ranging from autochthonous or parautochthonous to structurally higher nappe units. Mineralogically, they are dominated by vein quartz, minor calcite and chlorite and sulphides dominated by pyrrhotite. The lead isotope composition of the quartz vein mineralisation type [28] forms part of the same linear pattern as the fracture-controlled Zn-Pb deposits in the LSOD (Figure 15). These sulphide-bearing quartz veins, including those found in autochthonous positions near a nappe pile (e.g., Nasafjäll), are most likely of Caledonian origin and fluids may have infiltrated along thrust planes and faults [45]. However, considering the clear differences between these quartz veins and the basement-hosted Storuman fracture-controlled type with respect to tectonic setting, gangue mineralogy, and ore morphology alternative genetic models must be considered. The Caledonian quartz veins probably formed at higher temperatures and from less saline fluids than the fracture-controlled Zn-Pb deposits. For instance, fluid inclusions from quartz sulphide veins in the Olden area [46] indicate formation temperatures of at least 200–250 °C and salinities of 7–14 eq. mass% NaCl. Also, the physico-chemical depositional environment may have been different between sulphide-bearing calcite-veins and quartz veins [40].

The economically important Zn-Pb sandstone-hosted deposits (e.g., Vassbo and Laisvall; for location see inset in Figure 1) show many similarities with the fracture-controlled Zn-Pb type. Mineralisation occurs as cement in the sandstone and consists of sphalerite, galena, calcite, barite and fluorite. The lead isotope composition of these minerals is highly radiogenic and follows the same

linear trend as the LSOD Zn-Pb deposits (Figure 15). The ore-forming fluid had a salinity of 24 eq. mass% NaCl and a temperature of 150 °C [47], similar to the LSOD Zn-Pb ores. The prevailing view for the genesis of the sandstone-hosted deposits is that these are related to the reactivation of basement structures during the peak of the Caledonian orogeny [45].

5.6. Constraints on the Timing of Ore Formation

A number of hypothetical ore forming scenarios can be considered as mentioned earlier. The abundance of organic carbon, the Pb-Pb isotope pattern and lack of reasonable driving forces to induce fluid flow, suggest that neither Permian, nor Sveconorwegian processes led to the formation of the Zn-Pb deposits in the LSOD. This leaves two alternatives; either a Caledonian (Silurian thrusting) or a Cambrian (rifting) model.

Romer and Wright [27] have shown that Phanerozoic Pb mobilisation has occurred at several places within the Fennoscandian shield and they attributed this to tectonically induced fluid flow related to different orogenies. It is very likely that certain ore types in the Caledonides formed as a result of thrusting, but there is no *a priori* reason to claim that all ore types in settings near the Caledonides have the same origin and were formed at the same time. It should also be pointed out that there are no radiometric data available that directly constrain the Caledonian conceptual thrusting model for the genesis of the sandstone-hosted type. What is problematic in settings where mixing of fluids is inferred to have taken place is that any attempt to apply the isochron dating technique (e.g., Rb-Sr on sphalerite or Sm-Nd on scheelite) will probably produce scattered data. The reason behind the straight-line array in Figure 16 may be that the "cool" fluid precipitated abundant Ca-rich (and by inference Sr-rich) fluorite and calcite phases, which locally buffered the Sr isotope signature in the ore mineralising systems.

The genetic model presented here for the fracture-controlled Zn-Pb deposit type is similar to the basement reactivation model proposed by Romer and Wright [27] with a major difference being that the former ore deposits are considered to be due to a pre-Caledonian rifting event. Caledonian nappes probably covered the Ersmarksberget mineralisation and other studied occurrences (including the easternmost occurrence at Nyliden). In the light of a suggested pre-Caledonian model, one might expect clear evidence of post-mineralisation overprinting in the LSOD Zn-Pb ores as a result of Caledonian rocks being thrust onto the autochthonous Cambrian sequence. However, this is ruled out on the basis of pristine primary fluid inclusions in these ores. Sandstone-impregnated ores along the Caledonian margin, for which a pre-peak orogenic origin is locally indicated [3], exhibit similar fluid inclusions. As such inclusions are easily disturbed, there was probably no significant impact on the Rb-Sr systematics caused by the Caledonian orogeny.

Any suggested model for Pb-Zn ore formation requires fluid flow. In the LSOD this may have been caused by crustal thinning and rifting during opening of the Iapetus Ocean. This region is probably part of a rift basin preserved on the Baltic side of the rifted Rodinia continent, prior to establishment of a passive plate margin in Cambrian times. The existence of minor U, Mo, Ni and V occurrences in the Alum Shale [48] proves that mobilisation of fluids was an integral part of this evolution. Further evidence for hydrothermal event(s) preceding the Caledonian orogeny were presented by Sherlock *et al*. [49] who suggested, on the basis of ^{40}Ar-^{39}Ar data on K-feldspar overgrowths, that hydrothermal processes affected the ore-bearing sandstones at Laisvall at around 570–530 Ma ago.

Moreover, Romer and Wright [27] related certain radiogenic galenas to the formation of a *ca.* 450 Ma graben structure along the Gulf of Bothnia. These authors suggest initial formation of this graben in the Early Cambrian, and it makes sense to distinguish a 0.6–0.5 Ga rifting event that preceded the convergent phase in the Caledonian. Additional rift-related events include the Nb-Ta and Fe-mineralised Fen (539 ± 14 Ma) [50] and Alnö (590–580 Ma) carbonatite complexes [51,52].

5.7. A Preferred Genetic Model

Field, isotopic and fluid inclusion evidence supports a common genetic model for the fracture-controlled Zn-Pb mineralisation. Tentatively, there was a single ore-forming event characterised by similar features in the entire study area. For instance, mineralised drill intersections are very narrow within the sedimentary rocks and coincide with faults and related phenomena, and a strong structural control is indicated. There is no appreciable hydrothermal alteration around the ore-bearing structures. This lack of interaction with the wall rocks indicates development at a shallow crustal level, consistent with the low temperature ore fluids. Likewise, the presence of open spaces, crustiform veins, chalcedony, and marcasite/pyrite stalactites (gepetal structures) at Ersmarksberget, strongly suggests a very high (epithermal) level, probably within a few hundred metres of the original ground surface.

Considering the organic carbon in fluid inclusions and the inferred very shallow ore development, it is suggested that ore formation occurred after the deposition of black organic-rich Alum Shales (Mid-Late Cambrian) but before any Caledonian units were thrust over the mineralised sites. This view is consistent with the tentative Rb-Sr "isochron" age (534 ± 13 Ma). The mineralised Zn-Pb systems follow fractures, possibly failed rift arms of the early Iapetus Ocean [53], which extend down into the basement. Both fluid inclusion and isotope evidence support the hypothesis of minerals precipitating by mixing of two separate fluids at the site of Zn-Pb ore formation. These are referred to as the cool and the hot fluids and they show different salinities. The cool fluid was rich in Ca, by inference also in Sr, and comprises modified seawater with high salinity derived from water-mineral reactions within clay-rich sediments in a stagnant marine environment. This fluid, also carrying hydrocarbons and reduced sulphur, percolated downwards into the newly opened rift. A second fluid was simultaneously mobilised during rifting. This may also have had an ultimate marine origin, but as opposed to the cool fluid, it penetrated deeply into the basement. Thereby, it became heated and leached Pb, Zn, F and radiogenic Sr from the basement, which was dominated by K (Rb)-rich Revsund granite. By the time this fluid ascended, probably by convective circulation, it had been transformed into a relatively hot, metal-bearing fluid.

It is proposed that the hot ascending fluid met the cool fluid which was already in the rift structures. The pH during ore formation was weakly alkaline, given the stability of calcite and corrosion of early-formed quartz. Neither barite nor gypsum occurs in the LSOD deposits; their stability was probably inhibited by relatively low oxygen fugacity, as indicated by the organic material in the ore-forming fluids. The low abundance of pyrite and pyrrhotite also seems compatible with alkaline and low fO_2 conditions. Generally speaking, the sulphides (sphalerite and galena) were precipitated prior to the gangue minerals (calcite and fluorite). The fluid mixing on a local scale was also probably decisive for the isotope systematics. Taking Sr as an example, we suggest that sphalerites which

crystallized from an isotopically uniform ("cool") solution had a common Sr isotope ratio at the time of formation, and such samples would tend to form an isochron. In contrast, other sphalerites which indicate a range of initial Sr isotope ratios developed due to Sr-uptake through a variable mixing process between the cool and the hot fluid. The isotope systematics of lead and neodymium are less complex. Hypothetically, both these elements were essentially mobilised and transported by the hot fluid, and this governed partial isotope homogenisation as seen by fairly uniform initial Nd and Pb isotope compositions.

5.8. Is the Fracture-Controlled Zn-Pb Mineralisation in the LSOD Analogous to Mississippi Valley Type?

Sediment-hosted Pb-Zn deposits include a large group of ore mineralisation styles and genetic variants hosted by siliciclastic and carbonate rocks with no associated igneous activity [54]. The majority of the deposits occur in rift-related fault zones, commonly on the flanks of basins or in foreland thrust belts. Leach *et al*. [55] classified the sediment-hosted Pb-Zn deposits into three principal types: (i) synsedimentary to early diagenetic exhalative SEDEX type; (ii) epigenetic deposits hosted in platform carbonate sequences also referred to as the Mississippi Valley type (MVT); (iii) sandstone-hosted type. However, a continuum of subtypes exists between these types. For instance the MVT deposits encompass a wide range of ore styles (subtypes like Irish- and vein-type MVT) depending on the geological features (lithology and structures) that control fluid migration and sulphide-forming processes [54]. The deposits formed by similar depositional processes from migrating dense basinal metalliferous brines and with the Pb derived from a crustal source [56]. The ore fluids in all sediment-hosted Pb-Zn deposits share similar low temperatures (50–250 °C) and medium to high salinities (10–30 eq. mass% NaCl).

It is difficult to classify the LSOD Zn-Pb deposits as a typical sediment-hosted Pb-Zn deposit. The studied deposits show many similarities with MVT deposits such as an epigenetic mineralisation style, fracture-control, fluid characteristics, ore and gangue mineralogy, as well as the presence of bitumen. Nevertheless, there are obvious differences; most MVT deposits are hosted in platform carbonates, are stratabound, and occur in convergent settings. However, although the LSOD deposits are hosted by Early Proterozoic rocks, their inferred setting may actually be quite similar to that of MVT deposits. The following geological history is envisaged: (i) Neo-proterozoic-Cambrian platform sediments (locally including carbonates; [54]) were deposited on top of an eroded basement; (ii) ~530 Ma rifting/crustal attenuation generated extensional fractures and jogs in the basement which became mineralised by Zn-Pb-bearing ore fluids; (iii) nappe thrusting took place at ≥0.4 Ga; (iv) erosion removed the Caledonian nappes and autochthonous Cambrian rocks, leaving exposed mineralised basement. With regard to tectonic setting, a number of MVT deposits occur in extensional settings. There are examples described from Lennard Shelf of Australia [57] and Nanisvik in Canada [58], and this group also includes a number of MVT deposits from the eastern Alps and the Polish districts in Europe [59]. We therefore suggest that the LSOD mineralisation is a variety of MVT. The inferred Cambrian age for the LSOD deposits has few equivalents among the MVT family. Possible analogues of the same age include the Ediacara MVT deposit in south Australia where ore formation took place

during deposition of a Neocambrian-Cambrian sequence [60] and the MVT/SEDEX style deposits in northwest Queensland [61].

6. Conclusions

The Lycksele-Storuman Zn-Pb mineralisation occurs as veins and breccias that developed at shallow, epithermal depth. The mineralization was strongly controlled by contemporaneous strike-slip or transtensional faulting. The ores are similar to calcite vein mineralisation and economically important sandstone-impregnation Zn-Pb ores in the region. Two fluids of contrasting temperatures and salinities mixed at the site of ore deposition. They may both have been modified seawater fluids which upon mixing led to the precipitation of ore and gangue minerals. The mixing also led to complex Sr isotope systematics observed in the analysed minerals.

Ore formation took place during rifting, related to the opening of the Iapetus Ocean, and an MVT origin is suggested. The timing of ore formation is indicated by a 534 ± 13 Ma age, using the Rb-Sr method on sphalerite. Although the current Rb-Sr age needs to be substantiated by additional radiometric work, it appears that hitherto unknown, economic Cambrian base-metal mineralisation exists in the Fennoscandian shield.

Acknowledgements

We are indebted to Lappland Goldminers AB and Boliden Mineral AB for their support and their willingness to provide us with samples and company reports is greatly appreciated. Fredrik Grensman and Assen Simenov provided additional samples and introduced us to the geology at Ersmarksberget. The Swedish Geological Survey (SGU) kindly financed this project. The thorough and insightful comments from the journal reviewers are sincerely acknowledged.

References

1. Exploration Newsletter. Mineral Resources Information Office: Uppsala, Sweden. Available online: http://www.sgu.se/dokument/nyhetsbrev/exploration-newsletter-june-2006.pdf (accessed on 30 March 2012).
2. Kathol, B.; Weihed, P. Description of regional geological and geophysical maps of the Skellefte District and surrounding areas. In *Proceedings of the 26th Nordic Geological Winter Meeting*, Uppsala, Sweden, 6–9 January 2004; Abstract Volume.
3. Rickard, D.T.; Willdén, M.Y.; Marinder, N.E.; Donnelly, T.H. Studies on the genesis of the Laisvall sandstone lead-zinc deposit, Sweden. *Econ. Geol*. **1979**, *74*, 1255–1285.
4. Gáal, G.; Gorbatschev, R. An outline of the Precambrian evolution of the Baltic shield. *Prec. Res*. **1987**, *35*, 15–52.
5. Stephens, M.B.; Wahlgren, C-H.; Weihed, P. *Geological Map of Sweden, Scale 1:3 Million*; Geological Survey of Sweden: Uppsala, Sweden, 1994; Ba52.
6. Allen, R.L.; Weihed, P.; Svenson, S.-Å. Setting of Zn-Cu-Au-Ag massive sulfide deposits in the evolution and facies architecture of a 1.9 Ga marine volcanic arc, Skellefte District, Sweden. *Econ. Geol*. **1996**, *91*, 1022–1053.

7. Allen, R.L.; Weihed, P.; Blandell, D. Global comparision of volcanic-associated massive sulphide districts. *Geol. Soc. Lond. Spec. Publ.* **2002**, *204*, 13–37.
8. Bark, G.; Weihed, P. Orogenic gold in the new Lycksele-Storuman ore province, northern Sweden; the Palaeproterozoic Fäboliden deposit. *Ore Geol. Rev*. **2007**, *32*, 431–451.
9. Bergman-Weihed, J. Regional Deformation Zones in the Skellefte and Arvidsjaur Areas; Final Research Report, Geological Survey of Sweden: Uppsala, Sweden, 1997; Project 03–862/93.
10. Willdén, M.Y. Paleoenvironment of the autochthonous sedimentary rock sequence at Laisvall, Swedish Caledonides. *Stockholm Contrib. Geol.* **1980**, *23*, 1–100.
11. Moczydłowska, M.; Jensen, S.; Ebbestad, J.O.R.; Budd, G.E.; Martí-Mus, M. Biochronology of the autochthonous Lower Cambrian in the Laisvall-Storuman area, Swedish Caledonides. *Geol. Mag.* **2001**, *138*, 435–453.
12. Andersson, A.; Dahlman, B.; Gee, D.G.; Snäll, S. *The Scandinavian Alum Shales*; Geological Survey of Sweden: Uppsala, Sweden, 1985; Ca56, p. 50.
13. Gee, D.G.; Kumpulainen, R.; Thelander, T. *The Tåsjön Décollement, Central Swedish Caledonides*; Geological Survey of Sweden: Uppsala, Sweden, 1978; C74, pp. 1–35.
14. Bark, G. Gubbträsk—Översiktlig Borrkärnekartering; Company Report (in Swedish), Lappland Goldminers AB: Lycksele, Sweden, 2007; p. 11.
15. Eliasson, T.; Greiling, R.O.; Sträng, T.; Triumf, C-A. *Berggrundskartan 23H Stensele NO, Skala 1:50000*; Geological Survey of Sweden: Uppsala, Sweden, 2001; Ai127.
16. Bakker, R.J. Package Fluids 1. Computer programs for analysis of fluid inclusion data and for modelling bulk fluid properties. *Chem. Geol.* **2003**, *194*, 3–23.
17. De Ignacio, C.; Munoz, M.; Sagredo, J.; Fernandez-Santin, S.; Johansson, Å. Isotope geochemistry and FOZO mantle component of the alkaline-carbonatitic association of Fuerteventura, Canary Islands, Spain. *Chem. Geol*. **2006**, *232*, 99–113.
18. Schneider, J. Rb-Sr dating of epithermal vein mineralization stages in the eastern Harz Mountains (Germany) by paleomixing lines. *Geochim. Cosmochim. Acta* **2003**, *67*, 1803–1819.
19. Samson, I.M.; Walker, R.T. Cryogenic Raman spectroscopic studies in the system NaCl-$CaCl_2$-H_2O and implications for low-temperature phase behaviour in aqueous fluid inclusions. *Can. Mineral*. **2000**, *38*, 35–43.
20. Davis, D.W.; Lowenstein, T.K.; Spencer, R.J. Melting behaviour of fluid inclusions in laboratory-grown halite crystals in the systems NaCl-H_2O, NaCl-KCl-H_2O, NaCl-$MgCl_2$-H_2O, and NaCl-$CaCl_2$-H_2O. *Geochim. Cosmochim. Acta* **1990**, *54*, 591–601.
21. Oakes, C.S.; Bodnar, R.J.; Simonson, J.M. The system NaCl-$CaCl_2$-H_2O: I. The ice liquidus at 1 atm total pressure. *Geochim. Cosmochim. Acta* **1990**, *54*, 603–610.
22. Mullis, J.; Dubessy, J.; Poty, B.; O'Neil, J. Fluid regimes during late stages of continental collision: Physical, chemical, and stable isotope measurements of fluid inclusions in fissure quartz from a geotraverse through the Central Alps, Switzerland. *Geochim. Cosmochim. Acta* **1994**, *58*, 2239–2267.
23. Burke, E.A.J. Raman microspectrometry of fluid inclusions. *Lithos* **2001**, *55*, 139–158.
24. Pironon, J.; Barres, O. Semi-quantitative FT-IR microanalysis limits: Evidence from synthetic hydrocarbon fluid inclusions in sylvite. *Geochim. Cosmochim. Acta* **1990**, *54*, 509–518.

25. Wopenka, B.; Pasteris, J.D. Structural characterization of kerogens to granulite-facies graphite: Applicability of Raman microprobe spectroscopy. *Am. Mineral*. **1993**, *78*, 533–557.
26. Johansson, Å.; Rickard, D. Isotopic composition of Phanerozoic ore leads from the Swedish segment of the Fennoscandian Shield. *Miner. Depos*. **1984**, *19*, 249–255.
27. Romer, R.L.; Wright, J.E. Lead mobilization during tectonic reactivation of the western Baltic shield. *Geochim. Cosmochim. Acta* **1993**, *57*, 2555–2570.
28. Johansson, Å. Lead isotope composition of Caledonian sulphide-bearing veins in Sweden. *Econ. Geol.* **1983**, *78*, 1674–1688.
29. Billström, K.; Vivallo, W. Synvolcanic mixing of ore Pb and the development of lead isotopic provinces in the Skellefte district. *Miner. Depos.* **1994**, *29*,111–119.
30. De Paolo, D.J.; Linn, A.M.; Schubert, G. The continental crustal age distribution: Methods of determining mantle separation ages from Sm-Nd isotopic data and application to the Southwestern United States. *J. Geophys. Res.* **1991**, *96* (B2), 2071–2088.
31. Elming, S-Å.; Matsson, H.J. Post Jotnian basic intrusions in the Fennoscandian Shield, and the break up of Baltica from Laurentia: A paleomagnetic and AMS study. *Prec. Res*. **2001**, *108*, 215–236.
32. Björlykke, A.; Ihlen, P.M.; Olerud, S. Metallogeny and lead isotope data from the Oslo Paleorift. *Tectonophysics* **1990**, *178*, 109–126.
33. Leach, D.L.; Sangster, D.F. Mississippi Valley-Type lead-zinc deposits. In *Mineral Deposit Modelling*; Kirkham, R.V., Sinclair, W.D., Thorpe, R.I., Duke, J.M., Eds.; Geological Association of Canada: Newfoundland, Canada, 1993; Special Paper 40, pp. 289–314.
34. Moser, M.R.; Rankin, A.H.; Milledge, H.J. Hydrocarbon-bearing fluid inclusions in fluorite associated with the Windy Knoll bitumen deposit, UK. *Geochim. Cosmochim. Acta* **1992**, *56*, 155–168.
35. Kesler, S.E.; Jones, H.D.; Furman, F.C.; Sassen, R.; Anderson, W.H.; Kyle, J.R. Role of crude oil in the genesis of Mississippi Valley-type deposits: Evidence from the Cincinnati arch. *Geology* **1994**, *22*, 609–612.
36. Hübert, J.; Malehmir, A.; Smirnow, M.; Tryggvason, A.; Pedersen, L.B. MT measurements in the western part of the Paleoproterozoic Skellefte ore district/northern Sweden: A contribution to an integrated 3D geophysical study. *Tectonophysics* **2009**, *475*, 493–502.
37. Hooker, P.J.; Hamilton, P.J.; O'Nions, R.K. An estimate of the Nd isotopic composition of Iapetus seawater from *ca.* 490 Ma metalliferous sediments. *Earth Planet Sci. Lett*. **1981**, *546*, 180–188.
38. Johansson, Å. Fluid inclusion and stable isotope studies on some Caledonian sulphide-bearing veins in Sweden. *Econ. Geol*. **1984**, *79*, 1736–1748.
39. Welin, E.; Christiansson, K.; Kähr, A-M. Isotopic investigations of metasedimentary and igneous rocks in the Palaeoproterozoic Bothnian basin, central Sweden. *Geol. Soc. Stockh. Neg.* **1993**, *115*, 285–296.
40. Johansson, Å. Composition of sphalerite in some Swedish Pb-Zn-bearing veins. In *The Annual Report of the Ore Research Group*; Lindblom, S., Ed.; Stockholm University: Stockholm, Sweden, 1983; ORG-83, pp. 117–150.

41. Stephens, M.B. Stratabound sulphide deposits in the Central Scandinavian Caledonides. In *Proceeding of 7th IAGOD Symposium and Nordkalott Project Meeting Excursion Guide No.2*; Sveriges Geologiska Undersökning: Uppsala, Sweden, 1986.
42. Christofferson, H.C.; Wallin, B.; Selkman, S.; Rickard, D.T. Mineralisation controls in the sandstone lead-zinc deposit at Vassbo, Sweden. *Econ. Geol*. **1979**, *74*, 1239–1249.
43. Sundblad, K.; Zachrisson, E.; Smeds, S.A.; Berglund, S.; Ålinder, C. Sphalerite geobarometry and arsenopyrite geochemistry applied to metamorphosed sulfide ores in the Swedish Caledonides. *Econ. Geol*. **1984**, *79*, 1660–1668.
44. Sundblad, K.; Stephens, M.B. Lead isotope systematics of strata-bound sulphide deposits in the higher nappe complexes of the Swedish Caledonides. *Econ. Geol*. **1983**, *78*, 1090–1107.
45. Romer, R.L. Sandstone-hosted lead-zinc mineral deposits and their relation to the tectonic mobilization of the Baltic shield during the Caledonian orogeny—A reinterpretation. *Miner. Petrol*. **1992**, *47*, 67–85.
46. Sjöström, H.; Amcoff, Ö.; Broman, C.; Högdahl, K.; Rauséus, G. The Olden Window, Central Scandinavian Caledonides: Regional Structure and Local Sulphide Mineralisations in the Olden Area; Research Report of the Project "Replacement mineralisations Along the Storsjön-Edsbyn Deformation Zone", Geological Survey of Sweden: Uppsala, Sweden, 2004; Volume 4.
47. Lindblom, S. Textural and fluid inclusion evidence for ore deposition in the Pb-Zn deposit at Laisvall, Sweden. *Econ. Geol*. **1986**, *81*, 46–64.
48. Grenne, T.; Ihlen, P.M.; Vokes, F.M. Scandinavian caledonide metallogeny in a plate tectonic perspective. *Miner. Depos.* **1999**, *34*, 422–471.
49. Sherlock, S.C.; Lucks, T.; Kelly, S.P.; Barnicoat, A. A high resolution record of multiple diagenetic events: Ultraviolet laser microprobe Ar/Ar analysis of zoned K-feldspar overgrowths. *Earth Planet. Sci. Lett.* **2005**, *238*, 329–341.
50. Andersen, T.; Taylor, P.N. Pb isotope geochemistry of the Fen carbonatite complex, S.E. Norway: Age and petrogenetic implications. *Geochim. Cosmochim. Acta* **1988**, *52*, 209–215.
51. Andersen, T. Sr, Nd and Pb isotope data of the Alnö carbonatite complex. In *Proceedings of 22nd Nordic Geological Winter Meeting*, Turku, Finland, 1996; Abstract Volume, p. 11.
52. Meert, J.G.; Walderhaug, H.J.; Torsvik, T.H.; Hendriks, B.W.H. Age and paleomagnetic signature of the Alnø carbonatite complex (NE Sweden): Additional controversy for the Neoproterozoic paleoposition of Baltica. *Prec. Res*. **2007**, *154*, 159–174.
53. Kumpulainen, R.; Nystuen, J.P. Late Proterozoic basin evolution and sedimentation in the westernmost part of Baltoscandia. In *The Caledonide Orogen—Scandinavia and Related Areas*; Gee, D.G., Sturt, B.A., Eds.; John Wiley and Sons Ltd: Chicheste, UK, 1985; pp. 213–232.
54. Leach, D.L.; Bradley, D.C.; Huston, D.; Pisarevsky, S.A.; Taylor, R.D.; Gardoll, S.J. Sediment-hosted lead-zinc deposits in Earth History. *Econ. Geol*. **2010**, *105*, 593–625.
55. Leach, D.L.; Sangster, D.; Kelley, K.; Large, R.R.; Garven, G.; Allen, C.; Gutzmer, J.; Walters, S. Sediment-hosted lead-zinc deposits: A global perspective. *Econ. Geol*. **2005**, *100th Anniversary*, 561–607.
56. Leach, D.L.; Bradley, D.; Lewchuk, M.T.; Symons, D.T.A.; de Marsily, G.; Brannon, J. Mississippi Valley-type lead-zinc deposits through geological time: Implications from recent age-dating research. *Miner. Depos.* **2001**, *36*, 711–740.

57. Vearncombe, J.R.; Chisnall, A.W.; Dentith, M.C.; Dörling, S.L.; Rayner, M.J.; Holyland, P.W. Structural controls on Mississippi Valley type mineralization, the southeast Lennard shelf, Western Australia. In *Carbonate-Hosted Lead-Zinc Deposits*; Sangster, D.F., Ed.; Society of Economic Geologists: Littleton, CO, USA, 1996; Volume 4, pp. 74–95.
58. Symons, D.T.A.; Symons, T.B.; Sangster, D.F. Paleomagnetism of the society cliffs dolostone and the age of the Nanisivik zinc deposits, Baffin Island, Canada. *Mineral. Depos.* **2000**, *36,* 412–459.
59. Muchez, P.; Heijlen, W.; Banks, D.; Blundell, D.R.; Boni, M.; Grandia, F. Extensional tectonics and the timing and formation of basin-hosted deposits in Europe. In *Geodynamic and Ore Deposit Evolution in Europe*; Blundell, D.R., Arndt, N., Cobbold, P.R., Eds.; Gulf Professional Publishing: Oxford, UK, 2005; Volume 27, pp. 242–267.
60. Drew, G.J.; Both, R.A. The carbonate-hosted silver-lead deposits of the Ediacara mineral field, South Australia: Petrological, fluid inclusion and sulphur isotope studies. *Aust. J. Earth Sci.* **1984**, *31*, 177–201.
61. Cotter, S.J.; Moore, C.L.; Taylor, G.; Prince, K.E. Isotopic constraints on large-scale Sedex or MVT mineralization within the Cambrian carbonate cover sequences, northwest Qld. In *Regolith and Landscapes in Eastern Australia*; Roach, I.C., Ed.; CRC LEME: Canberra, Australia, 2002; pp. 14–16.